Holography : Non-contact and optical non-destructive testing applications

PASCAL PICART

05.28.2024

Table des matières

I.Présentation

Module :

Interference and diffraction

Auteur(s) :

Pascal PICART[1] - ENSIM – Le Mans Université

Résumé :

The lesson presents the methods of holographic, analogic and numerical interferometry. Sensibility notions, real time, intermediate time, stroboscopic measure are presented are presented and illustrated by concrete examples. Theoretical aspects proper to each method are also detailed. The case study gets onto the study of a cantilever beam by analogical holography.

Mots-clés :

Holography, Diffraction, Interferences, The Fresnel transform, Numerical hologram, Time average, Real time, Double exposition, Vibratory measure, Stroboscopic measure

Pré-requis :

Numerical and analogical holography, interferometry, inteferences, photometry basics

Objectif(s) pédagogique(s) :

To know the principles of analogical and numerical holographic interferometry methods

To be able to choose a holographic method to deal with a thin metrology problem in industry or in a laboratory

Plan du cours :

Conception & production :

Le Mans Université

Licence :

1 - pascal.picart@univ-lemans.fr
2 - http://www.gnu.org/licenses/fdl.txt

II.Course

The course on the methods of recording and reconstructing a holographically encoded object showed that all of the information pertaining to the object is contained in the reconstruction. Thus, it is natural to try to make a holographic object interfere with the initial object which has undergone deformations. Normally, in interferences between two waves, we see the appearance of fringes which are essentially caused by cosine modulation. This modulation is directly linked to the difference between the optical phase of the waves in interference. If an object wave interferes with the holographic wave of that object; the interferences between the two wave fronts will increase the variations in optical phase between the initial object and its reference. Using this method, it seems possible to study structures which have been subjected to pneumatic, thermal or mechanical stresses in a static, stationary or transitory system. This type of holography allows for a global evaluation which is both qualitative, through the simple visualisation of the fringes which code the deformation and quantitative through the data reduction of these fringes.

On the basis of this principle of interferences between object and hologram, it can be noted that anything which by nature is susceptible to undergoing a deformation, can, in principle, be analysed by holographic interferometry: from the deformation of an eardrum caused by a loud bang to the deformation of elements within an engine when it is in use, from the density variations of the air surrounding an aerofoil of an aeroplane's wing to the vibrations of a clarinet's reed when it is being played [1 [Holographie Industrielle]].

After 30 years of laboratory research, holographic interferometry is routinely used today in certain industrial sectors: modal analysis in the automobile and aeronautic industries, measuring deformations and validating calculation codes in the mechanics of solid objects, non destructive testing for large aeronautic structures such as certain elements of the Ariane missile or the ballistic missiles of the nuclear arsenal, the study of dynamic phenomena in vibratory mechanics, etc ... [2 [Holographic Interferometry – Principles and Methods]] It is a versatile technique, for example it gives as much qualitative visualisation for non destructive testing as it does for the stalling of engines.

This course presents the basic principles of the techniques for non-contact measurement and non destructive testing which are based on holographic interferometry.

1. Foreword

1.1. The notion of sensitivity vector

As was stated in the introduction, the basic avoidance of contact in holographic methods relies on the optical phase variation of the reconstructed object when it is subjected to a stress. This stress could be of a pneumatic, thermal, acoustic or mechanical nature.

The object, subjected to this stress, suffers a deformation, thus causing the optic path which is followed by the light on the journey *source-object-sensor* to change. Let's imagine a point A at the light source and a point B attached to the object. Normally, the optic path for the journey from point A to point B is defined by the following line integral :

$$(AB)=\int_A^B n\,ds$$

where $n$is the propagation environment index.

Figure 1 illustrates the possible journey for the optic path.

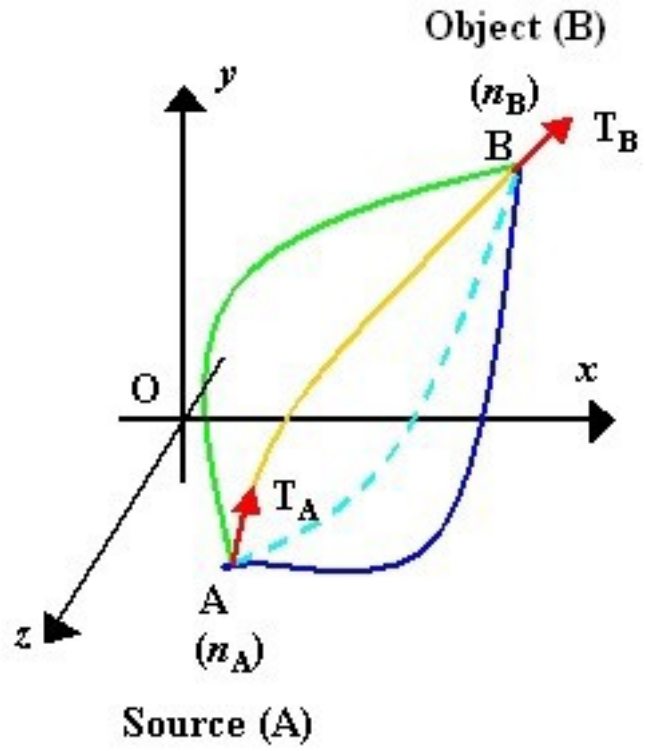

Figure 1 : Optical path

If the curve which symbolises the journey is slightly deformed, the integral (AB) is changed by a variation $\delta(AB)$ which is as infinite as the parameters which define the deformation. It is however possible to find curves for which $\delta(AB)$ is infinitesimally larger. Whatever the deformation of the optic journey, the integral (*AB*) is then stationary and the curve is said to be an extremal of the integral (AB). In this environment, the extremal curves, which effectively will be followed by the light, obey Fermat's principle: it can be shown that the path which is followed is such that the variation of the optical path is minimal, that is to say [3 [Principle of Optics]] :

$$\delta(AB) = n_B \mathbf{T_B}.\boldsymbol{\delta_B} - n_A \mathbf{T_A}.\boldsymbol{\delta_A} + \int_A^B \boldsymbol{\delta}\mathbf{M}.\left(\mathbf{grad}(n) - \mathbf{T}\frac{dn}{ds} - n\frac{d\,\mathbf{T}}{ds}\right)ds$$

with : n_A, n_B, T_A, T_B, δ_A, δ_B respectively being the indices, the tangents of the trajectory and the increments at the points A and B on the trajectory (AB). In the case where the object does not undergo a deformation, the curves pass constantly through points A and B so that the displacements δ_A and δ_B are always null. So that this expression might be equally null whatever the arbritary displacement $\delta\mathbf{M}$ which is printed at each point of the curve, it is evidently necessary to satisfy the following relationship

$$\mathbf{grad}(n) = \mathbf{T}\frac{dn}{ds} + n\frac{d\,\mathbf{T}}{ds}$$

Which fixes the extremal condition of the optical path (AB).

Let's consider the object in the context of a holographic experiment: the light comes from the source, meets the object and then is retro-diffused towards the sensor placed at point C (figure 2).

When the object is slightly deformed by a certain stress, point B (which is attached to the object) varies according to a three dimensional increment δ_B which causes variations in the optic path from A to B and from B to C. These variations are much smaller than the absolute values of these paths and have a modulus in the order of several tens or hundreds times the wave length of the light used for the illumination. The variation of the optic path is thus

$$\delta(ABC)=\delta(AB)+\delta(BC)$$

with

$$\delta(AB)=n_B\mathbf{T_B}.\boldsymbol{\delta_B}-n_A\mathbf{T_A}.\mathbf{0}$$

$$\delta(BC)=n_C\mathbf{T_C}.\mathbf{0}-n_B\mathbf{T'_B}.\boldsymbol{\delta_B}$$

Thus, we get

$$\delta(ABC)=n_B\mathbf{T_B}\boldsymbol{\delta_B}-n_B\mathbf{T'_B}\boldsymbol{\delta_B}=n_B\boldsymbol{\delta_B}.(\mathbf{T_B}-\mathbf{T'_B})$$

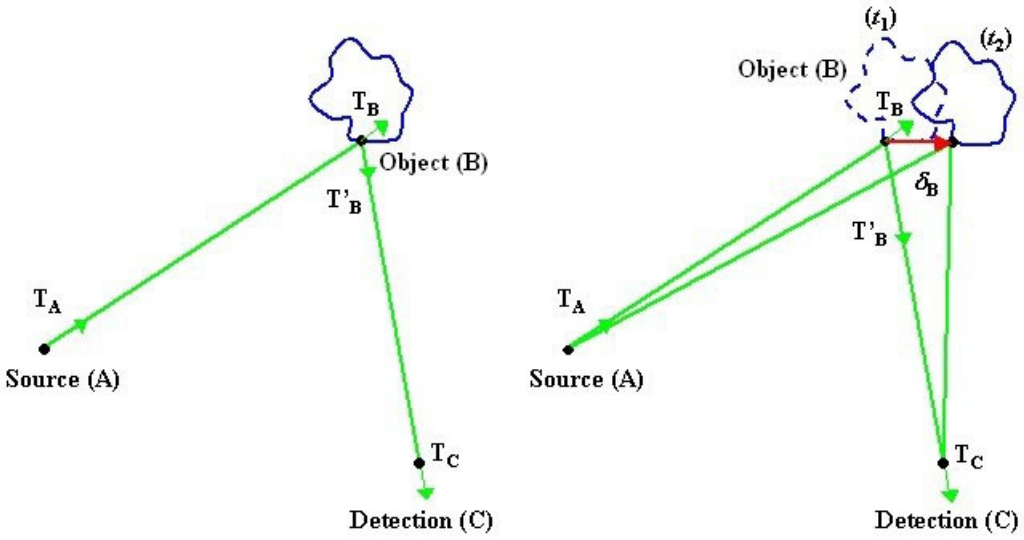

Figure 2 : Variation of the source-object-sensor-path

Note that $U = \delta_B$ is the vector for the displacement of the object caused by the stress which it is subjected to. Also note $K_e = T_B$ the vector for the "illumination" of the object, $K_0 = T'_B$ the vector for the "observation" of the object and $n$the index refractive index nearby the object [2 [Holographic Interferometry – Principles and Methods]].

The observation vector is linked to the observation direction from the object to the recording plate. The illumination vector represents the direction of illumination of the studied object.

Let's suppose :

$$\mathbf{S} = \mathbf{K_e} - \mathbf{K_o}$$

This vector is called the sensitivity vector. The sensitivity vector corresponds to the difference between the illumination vector and the vector for the observation of the object.

The sensitivity vector indicates the direction in which the sensitivity of the holographic device is optimum. It is essential to know the coordinates of this vector so that the metrologist can measure as precisely as possible the displacement amplitudes of an object.

The optical phase variation resulting from the variation of the *source-object-sensor* optical path is therefore given by the following relationship :

$$\Delta\varphi = \frac{2\pi n}{\lambda}\delta(ABC) = \frac{2\pi n}{\lambda}\mathbf{U}.\mathbf{S}$$

When the object is deformed, this results in the phase variation which is itself due to the variation of the optical path. This phase variation produces interference fringes which allow for the displacement of the object between two states to be quantified. The variation of the optical path seen by the acquisition system corresponds therefore to the variation of position of the object projected onto the sensitivity vector.

1.2. Interferences and sensitivity

Let's consider the object illuminated by the laser at a precise moment t_1, it is written :

$$A_1(x, y, t_1) = A_0(x, y)\exp(j\psi_0(x, y))$$

At a moment t_2, the object is subjected to a displacement caused by a certain stress which does not cause the object to be destroyed since the displacement is within the limits of what has been outlined above. It is therefore written :

$$A_2(x, y, t_2) = A_2(x, y)\exp(j\psi_2(x, y)) \approx A_0(x, y)\exp(j\psi_0(x, y) + j\Delta\varphi(x, y))$$

If the experimental device is capable of producing interferences between two objects at the two moments t_1 and t_2, then we would get a coherent superposition of the complex amplitudes leading to :

$$I(x, y, t_1, t_2) = A_0^2(x, y)(1 + \cos(\Delta\varphi(x, y)))$$

We would observe therefore the object modulated by a fringe signal linked to the optical phase variation between the two moments. These fringes are isodisplacement lines of the object between the two moments.

The stimulation which is applied to the object generally causes a displacement in three directions in the space behind $\mathrm{U} = u_x\mathrm{i} + u_y\mathrm{j} + u_z\mathrm{k}$. Note that depending on the orientation of the sensitivity vector, it is conceivable that the phase variation might be exclusively proportional to one of the displacement components, u_x, u_y or u_z or even proportional to a mixture of all the components.

1.3. The basics of holographic interferometry

Définition

Holographic interferometry is the term for all interference phenomenons in which at least one of the waves which creates the interference is produced by a hologram. Consequently, the most original characteristic of holographic interferometry is to permit interference by two contemporary waves. Even though interferometry normally applies to smooth waves it is in using two diffuse waves that the contribution of holography is unique: holography has the important secondary characteristic of being able to permit the interference of two neighbouring versions of the same diffuse wave.

In holographic interferometry, the observed interferences are characteristic of the micrometric displacements undergone by the object. Measuring the interferences allows the displacements to be quantified to an accuracy of a fraction of a micrometer.

Several methods of holographic interferometry exist, including the following examples :

- interferometry using a double-exposure [1 [Holographie Industrielle],2 [Holographic Interferometry – Principles and Methods],4 [Holographic Interferometry],5 [Interferometry With a Holographically Reconstructed Comparison Beam],6 [Dual and Multiple Beam Interferometry by Wavefront Reconstruction],7 [Interferometric Measurements on Diffuse Surfaces by holographic Techniques],8 [A Determination of the Optimum Beam Ratio to Produce Maximum Contrast Photographic Reconstructions from Double-Exposure Holographic Interferograms]]
- interferometry in real time [1 [Holographie Industrielle],2 [Holographic Interferometry – Principles and Methods],4 [Holographic Interferometry]]
- interferometry with time averaging [1 [Holographie Industrielle],2 [Holographic Interferometry – Principles and Methods],9 [Holographic Interferometry Applied to Measurements of Small Static Displacement of Diffusely Reflecting Surfaces]]
- interferometry with two reference beams [10 [Interferometric Analysis by Wavefront Reconstruction],11 [Two-Reference-Beam Holographic Interferometry]]
- digital holographic interferometry with time averaging [12 [Fringe Interpolation by Two-Reference-Beam Holographic Interferometry : Reducing Sensitivity to Hologram Misalignment],13 [Time-Averaged Digital Holography],14 [Some Opportunities for Vibration Analysis with Time-Averaging in Digital Fresnel Holography],15 [Dynamic Modal Characterization of Musical Instruments Using Digital Holography]]
- digital holographic vibrometry [16 [Time-Averaged In-Line Digital Holographic Interferometry for Vibration Analysis],17 [Full Field Vibrometry With Digital Fresnel Holography]]

Single reference beam holographic interferometry, which concerns the first three exaples, does not always allow for a quantitative study whereas interferometry with two reference beams allows quantitative studies in a more general manner. Digital holographic interferometry holds a particular place because it gives direct access to the optical phase variation caused by the displacement of the object. The following paragraphs tackle each of these methods.

2. Analogue holographic interferometry using of double-exposure

This technique is similar to that which is used to create a simple hologram. An initial exposure is carried out with the object in the first state then a second exposure onto the same photoplate with the object in the 2nd state [1 [Holographie Industrielle],2 [Holographic

Interferometry – Principles and Methods],4 [Holographic Interferometry],5 [Interferometry With a Holographically Reconstructed Comparison Beam],6 [Dual and Multiple Beam Interferometry by Wavefront Reconstruction],7 [Interferometric Measurements on Diffuse Surfaces by holographic Techniques],8 [A Determination of the Optimum Beam Ratio to Produce Maximum Contrast Photographic Reconstructions from Double-Exposure Holographic Interferograms]]. After development, we get a plate which contains the sum of the two holograms. At the reconstruction stage we get a superposition of two waves which come from the object in the 1st and 2nd states. These two waves interfere and the observed interference fringes translate the modification undergone by the object. The fringes are isoamplitude lines of the displacement. This method allows for the detection and the measurement of phase variations which occur between the two exposures.

2.1. Theoretical Aspect

Note O_1 and O_2 the complex amplitudes of the diffracted waves which come from the object in states 1 and 2. For each exposure we get

- during a time period Δt_1

$$H_1 = |R|^2 + |O_1|^2 + R^* O_1 + R O_1^*$$

- during a time period Δt_2

$$H_2 = |R|^2 + |O_2|^2 + R^* O_2 + R O_2^*$$

The energy received by the plate during the two exposures is

$$\begin{aligned} W &= \int_{t_1}^{t_1+\Delta t_1} H_1 dt + \int_{t_2}^{t_2+\Delta t_2} H_2 dt \\ &= (\Delta t_1 + \Delta t_2)|R|^2 + \Delta t_1 |O|_1^2 + \Delta t_2 |O_2|^2 + R^*(\Delta t_1 O_1 + \Delta t_2 O_2) + R(\Delta t_1 O_1^* + \Delta t_2 O_2^*) \end{aligned}$$

The transmission of the plate obtained after development is

$$t = t_0 - \beta R^* \left(\Delta t_1 O_1 + \Delta t_2 O_2\right) - \beta R \left(\Delta t_1 O_1^* + \Delta t_2 O_2^*\right)$$

During reconstruction using a laser as the light source, the amplitude transmitted by the plate is written

$$\begin{aligned} A_R &= R_t \\ &= Rt_0 - \beta |R|^2 (\Delta t_1 O_1 + Deltat_2 O_2) - \beta R^2 (\Delta t_1 O_1^* + \Delta t_2 0_2^*) \end{aligned}$$

As we saw in the course on recording and reconstruction :

- the first term corresponds to the 0-order
- the second term $-\beta |R|^2 (\Delta t_1 O_1 + \Delta t_2 O_2)$ corresponds to the $+1$-order
- the third term $-\beta R^2 (\Delta t_1 O_1^* + \Delta t_2 O_2^*)$ corresponds to the -1-order

Only the amplitude diffracted in the $+1$-order is of interest to us. The diffracted field in the $+1$-order at the distance $-d_0$ from the plate is therefore given by :

$$\begin{aligned} A_R^{+1}(x, y, -d_0, t_1, t_2) = &-\beta a_R^2 A_0(x, y) \exp\left(j \psi_0(x, y)\right) \\ &\times \left((\Delta t_1 + \Delta t_2) \exp\left(j \Delta \varphi(x, y)\right)\right) * \tilde{W}_A(x, y, -d_0) \end{aligned}$$

The image viewed by the observer is linked to the squared modulus of the diffracted field. By omitting the enlargement function $\tilde{W}_A(x, y, -d_0)$, we have

$$I_R^{+1}(x,y,-d_0,t_1,t_2)=\beta^2 a_R^4 A_0^2(x,y) \times\left(\Delta t_1^2+\Delta t_2^2+2\Delta t_1 \Delta t_2 \cos\left(\Delta\varphi(x,y)\right)\right)$$

It is an expression in the form

$$I_R^{+1}=I_0\left(1+m\cos\left(\Delta\varphi(x,y)\right)\right)$$

with

$$I_0=\beta^2 a_R^4\left(\Delta t_1^2+\Delta t_2^2\right) A_0^2(x,y)$$

$$m=\frac{2\Delta t_1 \Delta t_2}{\Delta t_1^2+\Delta t_2^2}$$

$$\Delta\varphi=\frac{2\pi n}{\lambda}\mathbf{U}.\mathbf{S}$$

Interferences are produced between the two virtual waves. These interferences modulate the image of the object and translate the phase variation which occurs between the first and second states. Most of the time it works out that $\Delta t_1 = \Delta t_2$ so that $m = 1$. The fringes therefore are contrasted to the maximum. These fringes firstly give a **qualitative information** on the displacement which have occurred. An adequate processing by computer allows a **quantitative analysis** by digitalisation of the image with a video camera or a digital camera.

2.2. The limitations of this procedure

The most notable limitations are the following :

- the amplitude of the displacement should lead to a number of resolvable fringes,
- the state of the object surface must not change from on exposition to another because if it did the fringe contrast would lower while the modification would increase,
- the holographic mounting, the object and the environment must remain stable during the length of each recording so that each corresponding hologram is of good quality.

2.3. The experimental set-up

The typical experimental configuration is off-axis and it is represented in figure 3. The light source must be spatially and temporally coherent except if a perfect balance between the object and reference optical paths can be assured.

An impulse laser can be used for the recording, which allows very short time delays in order to study objects under dynamic strain. The length of each exposure is the length of the laser impulse.

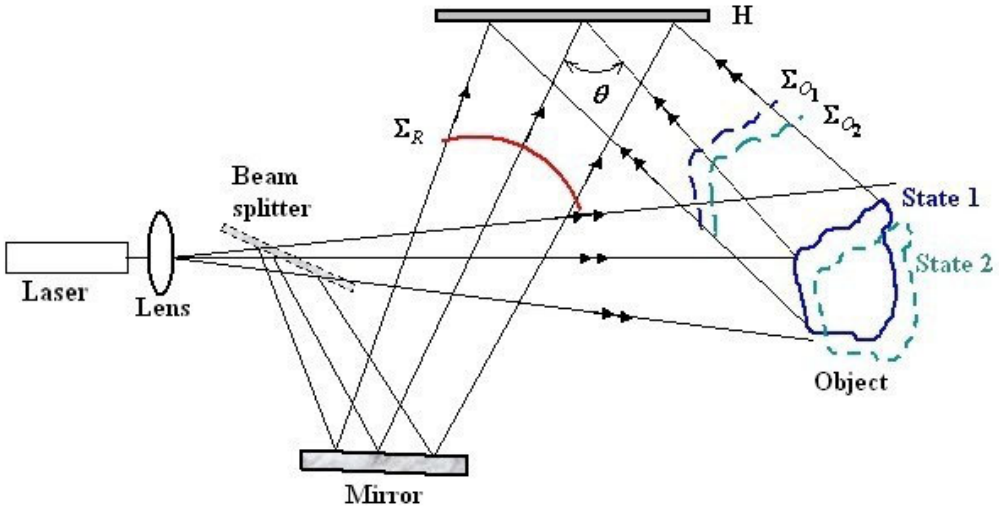

Figure 3 : Recording holograms by means of double exposition

Figure 4 shows the principal of reconstructing the two holograms by means of double exposure. The reconstructing laser can be continious wave with the same wave length as the recording laser. The observer can visualise the reconstructed object and the interference fringes which modulate its amplitude directly. However with an eye to the quantitative exploitation the visual observation is replaced by an observation using a camera or a video camera. It is sufficient to place the sighting of the lens towards the +1-order and to focus on the object.

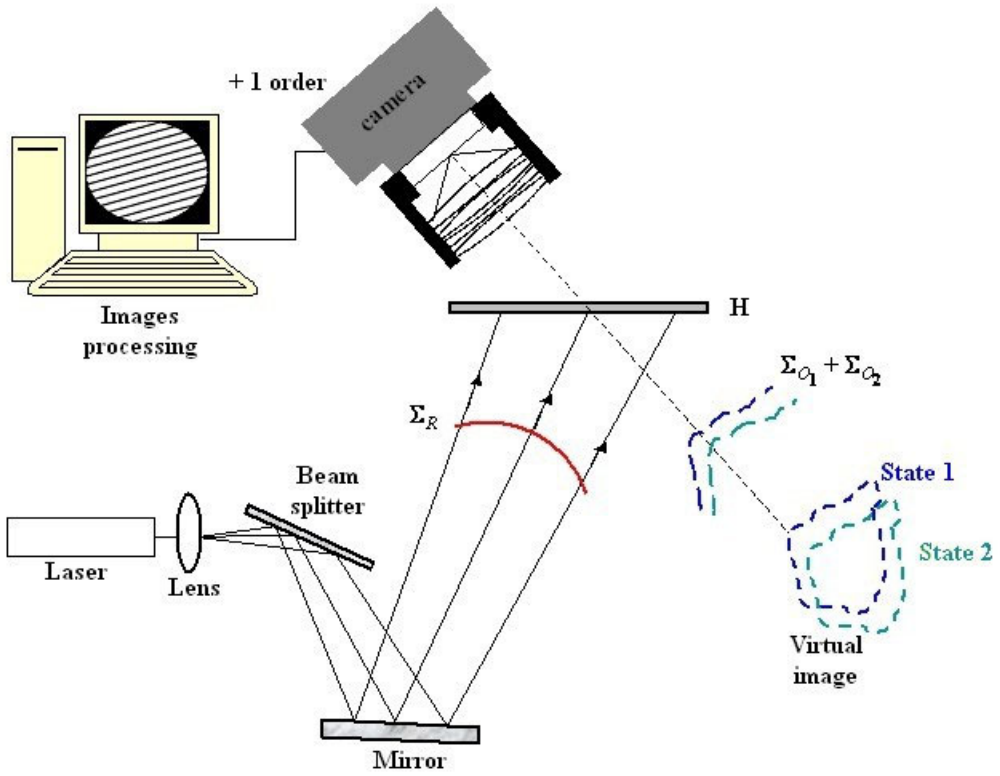

Figure 4 : Visualisation of holograms by double exposition

2.4. Applications and uses

This technique is applied in non-destructive testing in analysis of the mechanical, thermal or pneumatic constraints of an industrial object and equally in the analysis of defects in the object such as defects in the assembly of the object or structural cracks.

2.5. Illustration

In order to illustrate the above, figure 5 shows a double exposition hologram of a mechanical joint made of aluminium which is subjected to a force applied to its back panel. This is the view from above.

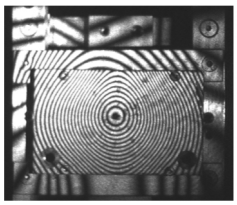

Figure 5 : Example of a double exposure hologram

The interference fringes which can be seen on the panel are interpreted as being lines of the isodeplacement of the structure. The symmetrical form of the fringes shows that the panel is not being subjected to a heavily anistrophic deformation.

3. Analogue holographic interferometry in real time

With a continuous laser beam a hologram of the object at rest is recorded. The photosensitive plate is developed then put back in **exactly** the same position in the mounting. The repositioning must be carried out to within a wave length. Then, at the same time the hologram is illuminated with the reference beam and the object is illuminated with the object [1 [Holographie Industrielle],2 [Holographic Interferometry – Principles and Methods],4 [Holographic Interferometry]].

Looking through the hologram we observe :

- the illuminated object
- the holographic image of the object

In the $+1$-order, interferences are produced between the wave diffracted in the $+1$-order and the wave which emanates from the object in its current state. If the object is moved or is deformed, interference fringes appear. The evolution of these fringes is followed in real time using the naked eye or using a rapid-shutter camera if the object's evolution is too rapid.

3.1. The Theoretical Aspect

The hologram is recorded when the object is in an initial state which can be its state when at rest. After the recording with an exposure time Δt, we get a transmission from the plate which is written,

$$t = R\,t_0 - \beta\,\Delta t\,|R|^2 O - \beta\,\Delta t\,R^2 O^*$$

And the diffracted field in the $+1$-order at the distance $-d_0$ from the plate is given by :

$$A_R^{+1}(x,y,-d_0)=-\beta\,\Delta t\,a_R^2\,A_0(x,y)\exp(j\,\psi_0(x,y))*\widetilde{W}_A(x,y,-d_0)$$

Note $A_i$the instantaneous complex amplitude emanating from the real object illuminated by the laser.
We can write

$$A_i(x,y,t)=A_i(x,y)\exp(j\,\psi_i(x,y))\approx A_0(x,y)\exp(j\,\psi_0(x,y)+j\,\Delta\varphi(x,y,t))$$

Where the phase variation depends on the time if the object undergoes a displacement

$$\Delta\varphi(t)=\frac{2\pi n}{\lambda}\mathbf{U}(t).\mathbf{S}$$

During the observation of the $+1$-order, there is a superposition of the diffracted amplitude and of the amplitude emanating from the object after going through the photosensitive plate. Thus, we get

$$A_T^{+1}(x,y,t)=t_0\,A_i(x,y,t)+A_T^{+1}(x,y,-d_0)$$

Which, by omitting the enlargement function. $\tilde{W}_A(x,y,-d_0)$ is equally written,

$$A_T^{+1}(x,y,t)=A_0(x,y)\exp(j\,\psi_0(x,y))\left(-\beta\,\Delta t\,a_R^2+t_0\exp(j\,\Delta\varphi(x,y,t))\right)$$

The image seen by the observer is linked to the squared modulus of the diffracted field. We get

$$I_T^{+1}(x,y,t)=A_0^2(x,y)\left(\beta^2\Delta t^2\,a_R^4+t_0^2-2\,\beta\,t_0\,\Delta t\,a_R^2\cos(\Delta\varphi(x,y,t))\right)$$

It is an expression in the form

$$I_R^{+1}(t)=I_0\left(1-m\cos(\Delta\varphi(x,y,t))\right)$$

with

$$I_0=A_0^2(x,y)\left(\beta^2\Delta t^2\,a_R^4+t_0^2\right)$$

$$m=\frac{2\,\beta\,t_0\,\Delta t\,a_R^2}{\beta^2\Delta t^2\,a_R^4+t_0^2}$$

Interferences are produced in the $+1$-order. If the object is immobile, we observe its image with an amplitude equal to $(1-m)I_0$, which constitutes a flat tint. In the case where $m = 1$, the image is dark ; however, this case is rare in practice because it is difficult to adjust the two amplitudes so that $t_0=\beta\Delta a_R^2$. If the object is deformed by an ordinary stress, the phase variation would be non-zero and we would see interference fringes which evolve with the stress applied to the object.

3.2. The Limitations of this procedure

The principal limitation as far as this analysis technique is concerned comes from the fact that the photosensitive plate needs to be replaced in the mounting after its development. This adjustment needs to be highly precise and requires an isostatic mechanical device.

Indeed, if the hologram is replaced in the mounting with a lateral discrepancy, the virtual object would be equally shifted and could not be superimposed on the real object. If the discrepancy is not too great you get parasitic fringes or the appearance of two spatially staggered objects if the discrepancy is very large.

To get round this inconvenience, thermoplastic films can be used for rapid development in situ.

Other notable limitations are :

- the amplitude of the displacement should lead to a number of resolvable fringes,
- The state of the object surface must not change from on exposition to another because if it did the fringe contrast would lower while the modification would increase.

3.3. The Experimental Set-up

The experimental device is conventional since it is being used to record a hologram of an object at rest (figure 6). The light source must equally be spatially and temporally coherent except if a perfect balance between the object and the reference optical paths can be assured.

An impulse laser can also be used for the recording, which allows for very short exposure times.

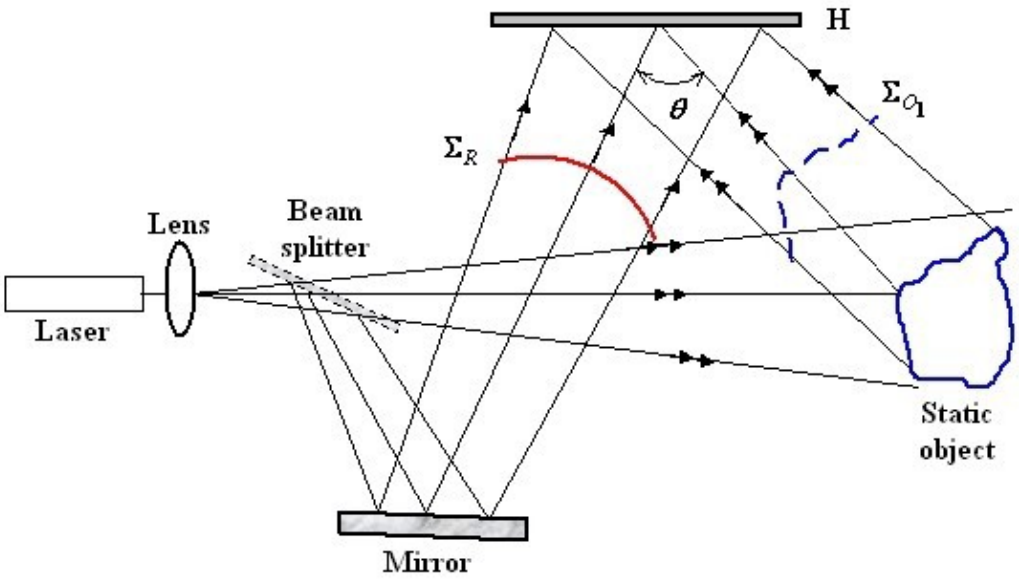

Figure 6 : Recording holograms for the real time method

Figure 7 shows the principle of the real time method. At the same time, the hologram is illuminated with the reference beam and the object is illuminated with the object beam. The reference beam diffracts onto the hologram and reconstructs the previously recorded object. At the same time, the object beam illuminated he real object and this then interferes with the virtual wave reconstructed by diffraction. The observer can directly visualise he reconstructed object and the interference fringes which modulate its amplitude. However, with a view to a quantitative exploitation, visual observation is replaced with an observation using a camera or a video camera. It is sufficient to place the sighting of the lens towards the $+1$-order and to focus on the object as shown in figure 7.

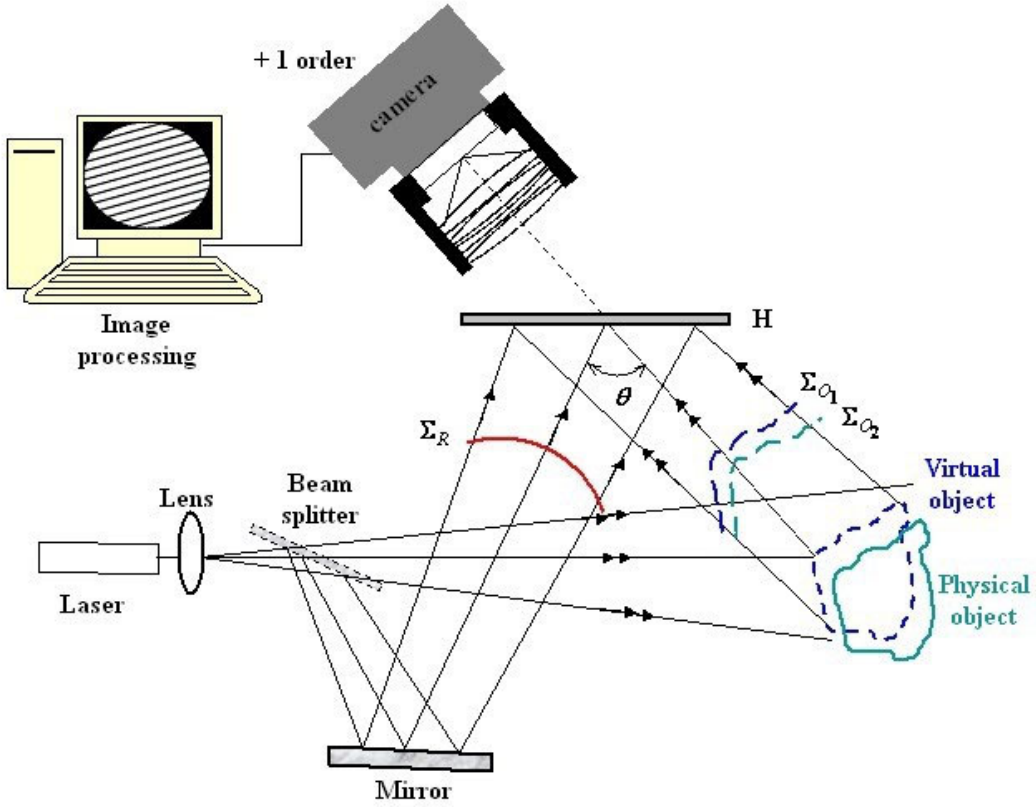

Figure 7 : Visualisation in real time

3.4. Applications and uses

Interferometry in real time is used for non-destructive testing, vibratory analysis or even to understand the entirety of the behaviour of mechanical structures submitted to static or slowly changing constraints.

Exemple

For example : the deformation of the casing of a gearbox when the shaft torque is slowly changed ; the detection of defects when a thermal constraint is developed, etc...

3.5. Illustration

Figure 8 illustrates the appearance of fringes in real time when a composite membrane in which an adhesion defect is present is tested with a thermal source.

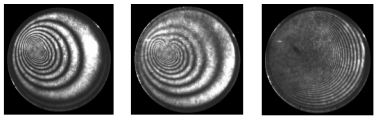

Figure 8 : Example of holograms in real time

When the thermal constraint is increased the number of fringes increases until it is impossible to distinguish them because they are too tightly packed together as the image on the right shows.

3.6. The particular case of an object in harmonic vibration

A case is often encountered in practice when the object is subjected to a harmonic constraint which is not "slow" in comparison to the observation process.
In this case the displacement vector is of the form

$$\mathbf{U}(t)=\mathbf{U_0}\sin(\omega_0 t+\varphi_0)$$

The instantaneous phase variation is written

$$\Delta\varphi(t)=\frac{2\pi}{\lambda}\mathbf{U_0}.\mathbf{S}\sin(\omega_0 t+\varphi_0)$$

The image observed in the $+1$-order at each moment is written

$$I_R^{+1}(t)=I_0\left(1-m\cos\left(\Delta\varphi_0\sin(\omega_0 t+\varphi_0)\right)\right)$$

with

$$\Delta\varphi_0=\frac{2\pi}{\lambda}\mathbf{U_0}.\mathbf{S}$$

The observation, be it visual or optoelectronic, is carried out with an exposure time $\Delta\tau$. For vibrating objects with frequencies greater than $1/\Delta\tau$there follows a temporal integration of the signal $I_R^{+1}(t)$.
The signal actually seen by the observer is therefore given by

$$\Delta I_R^{+1}=\int_{t_1}^{t_1+\Delta\tau} I_R^{+1}(t)\,dt$$

As $I_R^{+1}(t)$ develops in a series of Bessel functions, we also get

$$I_R^{+1}(t)=I_0-m I_0 J_0(\Delta\varphi_0)-2m I_0\sum_{n=1}^{\infty} J_{2n}(\Delta\varphi_0)\cos(2n\omega_0 t+2n\varphi_0)$$
$$+2m I_0\sum_{n=0}^{\infty} J_{2n+1}(\Delta\varphi_0)\sin((2n+1)\omega_0 t+(2n+1)\varphi_0)$$

And the temporal integration gives

$$\Delta I_R^{+1}=I_0\Delta\tau-m I_0\Delta\tau J_0(\Delta\varphi_0)-2m I_0\Delta\tau\sum_{n=1}^{\infty} J_{2n}(\Delta\varphi_0)\,\mathrm{sinc}(n\omega_0\Delta\tau)\cos(2n\omega_0 t_1+2n\varphi_0)$$
$$+2m I_0\Delta\tau\sum_{n=0}^{\infty} J_{2n+1}(\Delta\varphi_0)\,\mathrm{sinc}\left(\frac{2n+1}{2}\omega_0\Delta\tau\right)\sin((2n+1)\omega_0 t_1+(2n+1)\varphi_0)$$

If the exposure time of the observation is such that $\omega_0\Delta\tau \gg 1$
We get

$$\mathrm{sinc}(n\omega_0\Delta\tau)\approx 0\ \forall\ n$$
$$\mathrm{sinc}\left(\frac{2n+1}{2}\omega_0\Delta\tau\right)\approx 0\ \forall\ n$$

It therefore becomes

$$\Delta I_R^{+1} \approx I_0 \Delta\tau \left(1 - m J_0(\Delta\varphi_0)\right)$$

The expression of the interference signal shows that the amplitude of the reconstructed object is modulated by the function $1 - mJ_0(\Delta\varphi_0)$ which depends on the contrast between the two waves and the Bessel function J_0. The value of the Bessel function depends on the amplitude of the object's vibration via the phase $\Delta\varphi_0$. Figure 9 shows the profile of the fringes for $\Delta\varphi_0$ varying from 0 to 10π and for $m = 0.1\,;0.25\,;0.5\,;0.75\,;1$. The modulating function has a contrast which depends on m as is illustrated in figure 9.

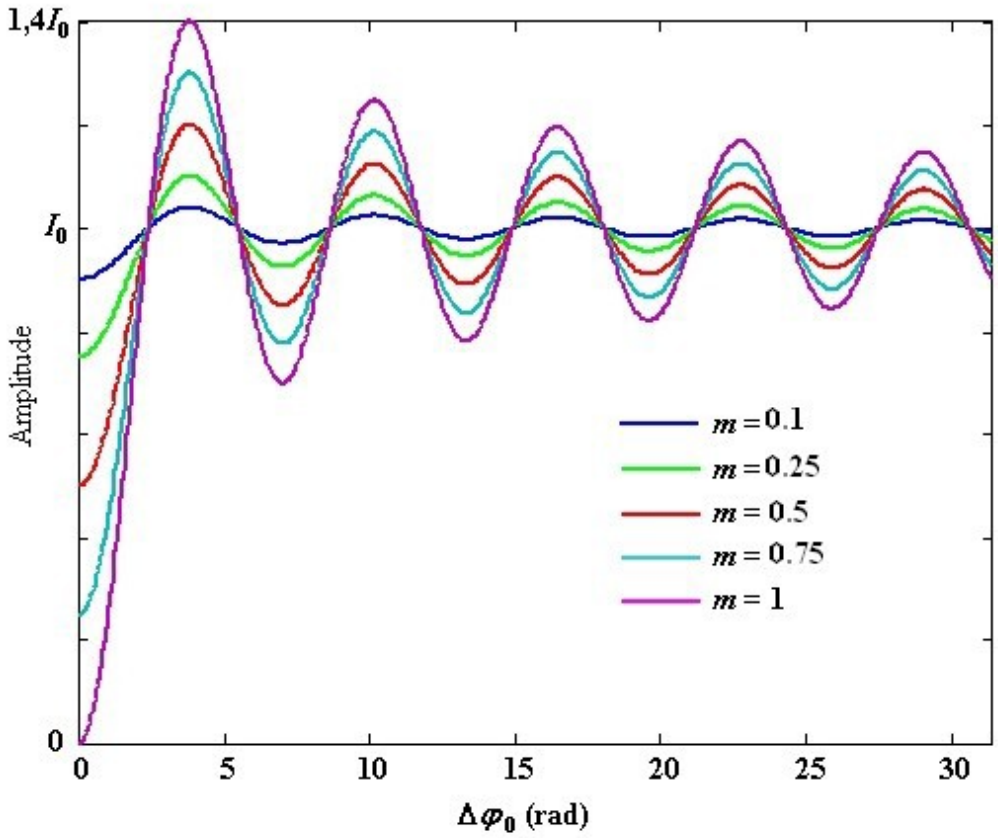

Figure 9 : Modulating function of the reconstructed hologram

The contrast of the fringes is in any case much lower than the contrast of the whole. When the two object waves are such that $m = 1$, the **dark fringes** for which $\Delta I_R^{+1} = 0$correspond to the zones of the object which remain immobile during the sinusoidal oscillation ; they therefore correspond to the **nodal lines** of the object.

It can also be noted that the expression ΔI_R^{+1} does not include the vibratory phase φ_0. The information concerning the vibration displacement is therefore lost by this process. It is one of the principal properties of the methods based on the temporal integration of harmonically oscillating phenomena and it is to be seen in every technique of holography by temporal integration.

Figure 10 shows holograms observed in real time when the object is sinusoidally stimulated.

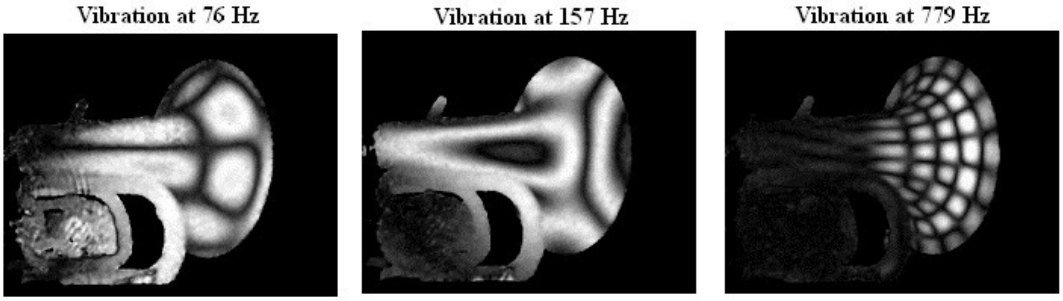

Figure 10 : Example of hologram in real time and temporal integration

The dark fringes correspond to the nodal lines of the object.

4. Analogue interferometry with time averaging

This method is also known as holographic interferometry by temporal integration. The principal use of this method is in the vibration analysis of structures. The principle is simple: in a classic holographic mounting the hologram of the vibrating object is recorded with an exposure time which is long in comparison with the period of vibration [1 [Holographie Industrielle],2 [Holographic Interferometry – Principles and Methods],9 [Holographic Interferometry Applied to Measurements of Small Static Displacement of Diffusely Reflecting Surfaces]]. The method allows for the carthography of the periodically vibrating object's amplitude to be visualised along with its nodal lines.

In the $+1$-order, the diffracted wave is modulated by a function which depends exclusively on the amplitude of the vibration.

4.1. Theoretical Aspect

The hologram is recorded when the object is harmonically stimulated. In order to clarify the principle of the image formation, let's consider that the object is stimulated in a purely sinusoidal excitation. As we have seen previously , the displacement vector of the object takes the form

$$\mathbf{U}(t)=\mathbf{U_0}\sin(\omega_0 t+\varphi_0)$$

And the instantaneous phase variation is written

$$\Delta\varphi(t)=\Delta\varphi_0\sin(\omega_0 t+\varphi_0)$$

The wave diffracted by the object towards the photosensitive plate depends on the time through the following relationship :

$$O(x',y',d_0,t)=-\frac{j\exp(2j\pi d_0/\lambda)}{\lambda d_0}\exp\left(\frac{j\pi}{\lambda d_0}(x'^2+y'^2)\right)$$
$$\times\int_{-\infty}^{+\infty}\int_{-\infty}^{+\infty}A(x,y,t)\exp\left(\frac{j\pi}{\lambda d_0}(x^2+y^2)\right)\exp\left(-\frac{2j\pi}{\lambda d_0}(xx'+yy')\right)dxdy$$

with

$$A(x,y,t)=A_0(x,y)\exp(j\psi_0(x,y))\exp\left(j\Delta\varphi_0(x,y)\sin(\omega_0 t+\varphi_0(x,y))\right)$$

And the instantaneous hologram also depends on the time

$$H(t)=|R|^2+|O(t)|^2+R^*O(t)+RO^*(t)$$

The energy received by the plate during the exposure is

$$\begin{aligned} W &= \int_{t_1}^{t_1+\Delta t} H(t)dt \\ &= \Delta t|R|^2 + \int_{t_1}^{t_1+\Delta t} |O(t)|^2 dt + R\int_{t_1}^{t_1+\Delta t} O^*(t)dt + R^*\int_{t_1}^{t_1+\Delta t} O(t)dt \end{aligned}$$

The last term will from the $+1$-order during the process of reconstruction by laser diffraction. Taking into account results given in the course on the formation of images, the diffracted amplitude in the $+1$-order is written, by omitting the spatial dependency (x,y),

$$A_R^{+1}(-d_0)=-\beta\, a_R^2\{\int_{t_1}^{t_1+\Delta t} A_0\exp(j\psi_0)\exp\left(j\Delta\varphi_0\sin(\omega_0 t+\varphi_0)\right)\,dt\}*\widetilde{W}_A(-d_0)$$

Which is also to say

$$A_R^{+1}(-d_0)=-\beta\, a_R^2\{A_0\exp(j\psi_0)\int_{t_1}^{t_1+\Delta t} \exp\left(j\Delta\varphi_0\sin(\omega_0 t+\varphi_0)\right)\,dt\}*\widetilde{W}_A(-d_0)$$

Since

$$\exp\left(j\Delta\varphi_0\sin(\omega_0 t+\varphi_0)\right)=\sum_{n=-\infty}^{n=+\infty} J_n(\Delta\varphi_0)\exp\left(jn(\omega_0 t+\varphi_0)\right)$$

The temporal integration of the complex term leads to

$$\int_{t_1}^{t_1+\Delta t}\exp\left(j\Delta\varphi_0\sin(\omega_0 t+\varphi_0)\right)dt=\Delta t\sum_{n=-\infty}^{n=+\infty} J_n(\Delta\varphi_0)\operatorname{sinc}\left(n\omega_0\frac{\Delta t}{2}\right)\exp\left(jn\omega_0\frac{\Delta t}{2}\right)\exp\left(jn(\omega_0 t_1+\varphi_0)\right)$$

If the length of recording the hologram is such that $\omega_0\Delta t \gg 1$
then we get

$$\operatorname{sinc}\left(n\omega_0\frac{\Delta t}{2}\right)\approx 0\ \forall\ n$$

It thus follows that

$$\int_{t_1}^{t_1+\Delta t}\exp\left(j\Delta\varphi_0\sin(\omega_0 t+\varphi_0)\right)dt\approx\Delta t\, J_0(\Delta\varphi_0)$$

The image in the $+1$-order seen by the observer is linked to the squared modulus of the diffracted field. By leaving out the enlargement function $\tilde{W}_A(x,y,-d_0)$, we get

$$I_R^{+1}(x,y,-d_0)=|A_R^{+1}(x,y,-d_0)|^2$$
$$=\beta^2 a_R^4 \Delta t^2 A_0^2(x,y)|J_0(\Delta\varphi_0(x,y))|^2$$

It is an expression in the form

$$I_R^{+1}=I_0|J_0(\Delta\varphi_0)|^2$$

The expression of the image in the $+1$-order shows that the reconstructed object is modulated by the Bessel function $|J_0|^2$. The value of the Bessel function depends on the vibration amplitude of the object through the optical phase $\Delta\varphi_0$. Figure 11 shows the fringe profile for $\Delta\varphi_0$ varying from 0 to 10π.

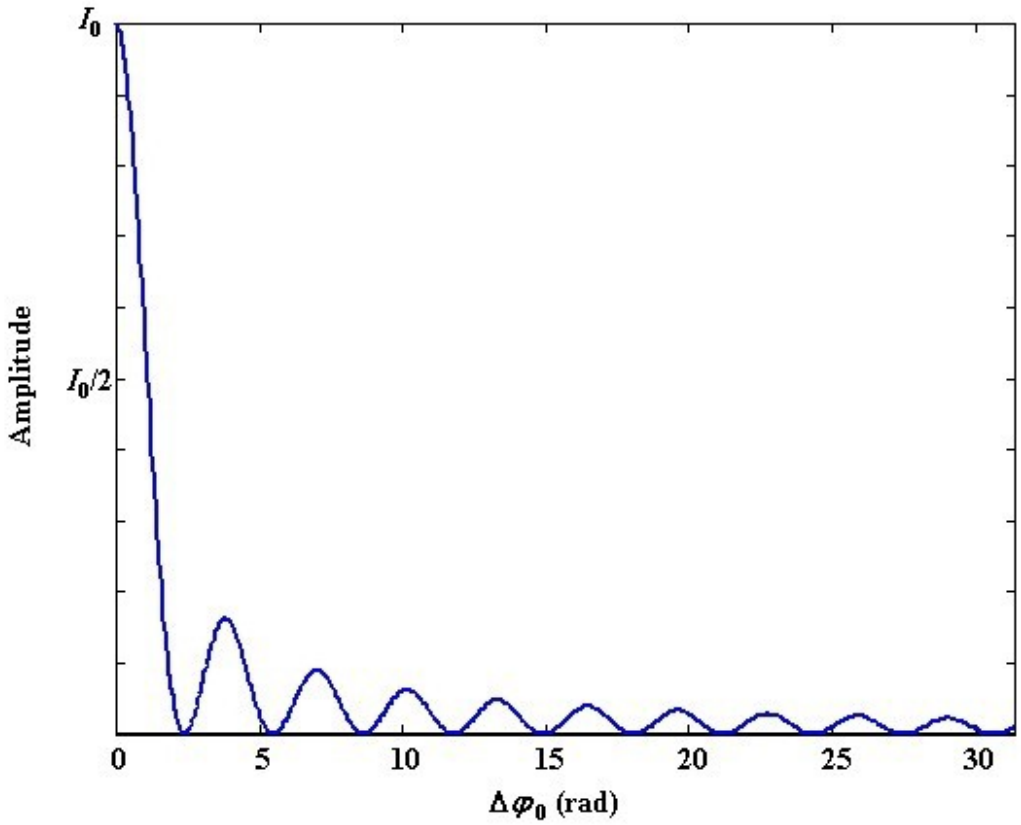

Figure 11 : Modulation function with time averaging

The modulation function is maximum for $\Delta\varphi_0 = 0$ which corresponds to the object zones which stay still during the sinusoidal oscillation. Thus, the **shining fringes** for which $I_R^{+1} = I_0$ correspond to the **nodal lines** of the object. When the vibration amplitude increases, the Bessel function gets smaller and is cancelled out for certain values, notated ω_n. When the Bessel function is cancelled out, a dark fringe can be seen since the image shows a null minimum. The secondary oscillations of the Bessel function have an amplitude which decreases progressively so that the dark fringes show less and less contrast. As has already been noted in the study of the real time interferometric method, I_R^{+1} does not include the vibration phase φ_0 .

Table 1 sums up the values of the zeros $\omega_n$of the function J_0.

Order n	Zeros ω_n (rad)
1	2.40
2	5.52
3	8.65
4	11.79
5	14.93
6	18.07
7	21.21
8	24.35
9	27.49
10	30.63
11	36.92
12	40.06

Table 1 : Table of zeros of the Bessel modulation

4.2. The limitations of this procedure

The temporal integration technique requires the use of a continuous walse laser with what can be long exposure times, depending on the available laser flux. The recording conditions are the same as those for a classic hologram: a stable mounting on an anti-vibration table. Precautions must also be taken that the vibration of the structure does not cause parasitical displacements of the whole structure.

4.3. The experimental set-up

The experimental system is the classic holographic system since it comes down to recording a hologram of the object (see figure 6). However, the object must be sinusoidally stimulated by a vibration source which can be a loud speaker (acoustic stimulation) or a vibrometer (mechanical stimulation).

4.4. Applications and uses

This technique, associated with the real time technique, is very useful for the analysis of vibratory modes of industrial structures: modal analysis, certification of calculation codes, etc...

4.5. Illustration

Figures 12 to 14 show the Bessel fringes obtained during the excitation of a composite membrane by a loud speaker placed on its back for excitation frequencies of 980 Hz, 1180 Hz, 1300 Hz, 2110 Hz and 2200 Hz respectively.

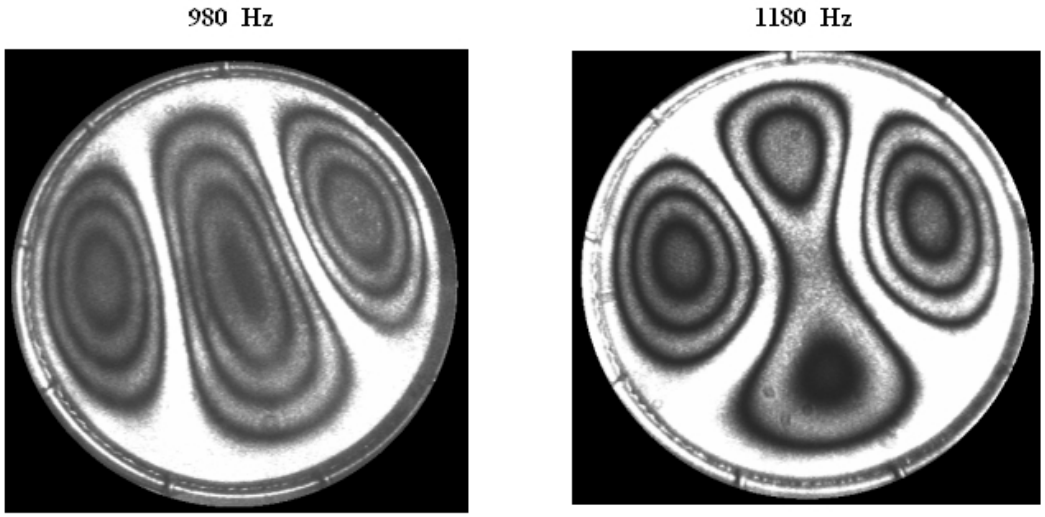

Figure 12 : Time averaged hologram at 980Hz and 1180Hz

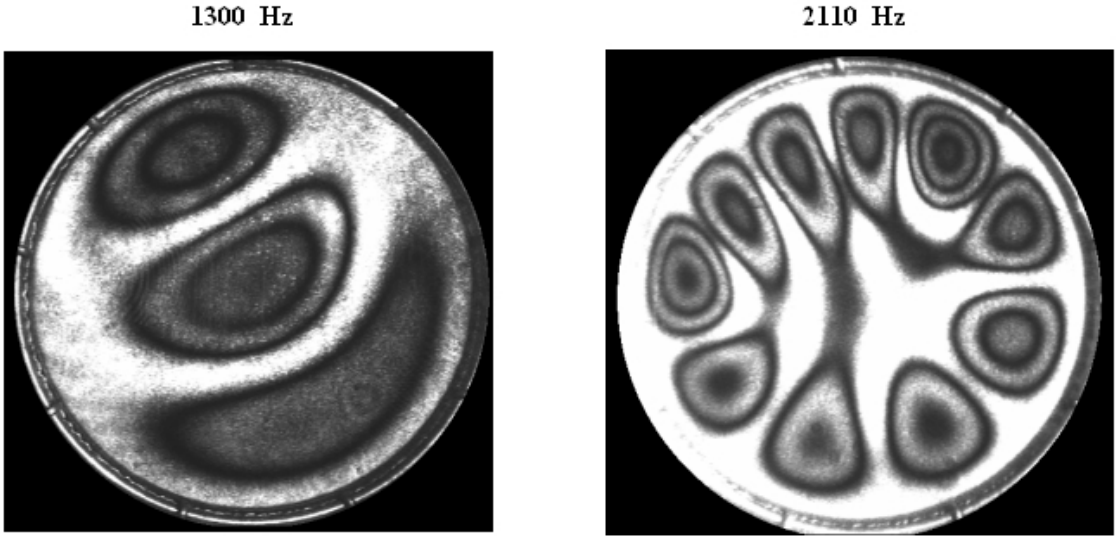

Figure 13 : Time averaged hologram at 1300Hz and 2110Hz

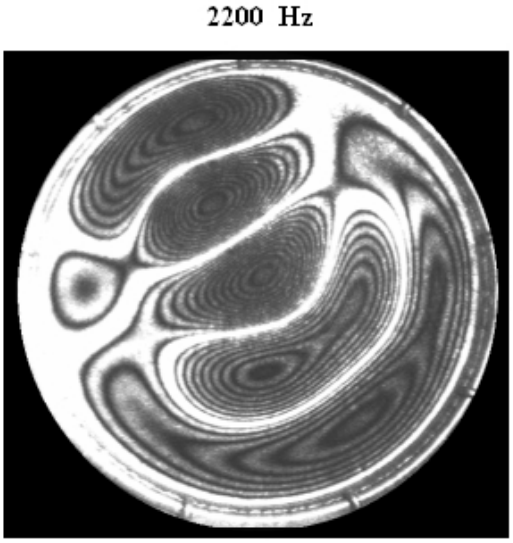

Figure 14 : Time averaged hologram at 2200Hz

The time averaging method can equally be used to detect structural defects. Indeed, the presence of a defect would change the modal structure of the vibration. By comparison with the vibratory signature of a healthy structure, invisible and hidden modifications and defects can be identified.

Figure 15 depicts this possibility by showing two modal signatures obtained with a stimulus of $1180\ \mathrm{Hz}$ for a healthy structure and for a defected structure.

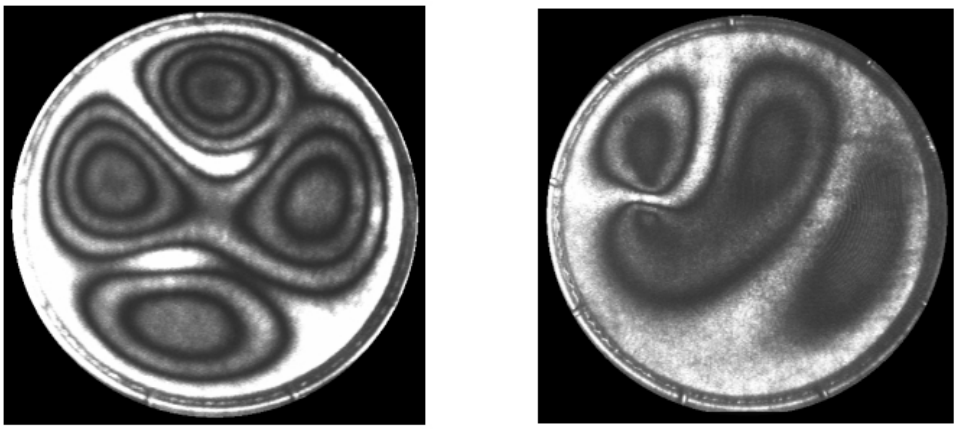

Figure 15 : The modal signatures at 1180Hz for healthy and defected structures

The presence of a defect (on the right) can easily be observed as well as the modification of the modal structure which this causes.

Figure 16 illustrates the influence of a defect for a stimulus of $1820\ \mathrm{Hz}$.

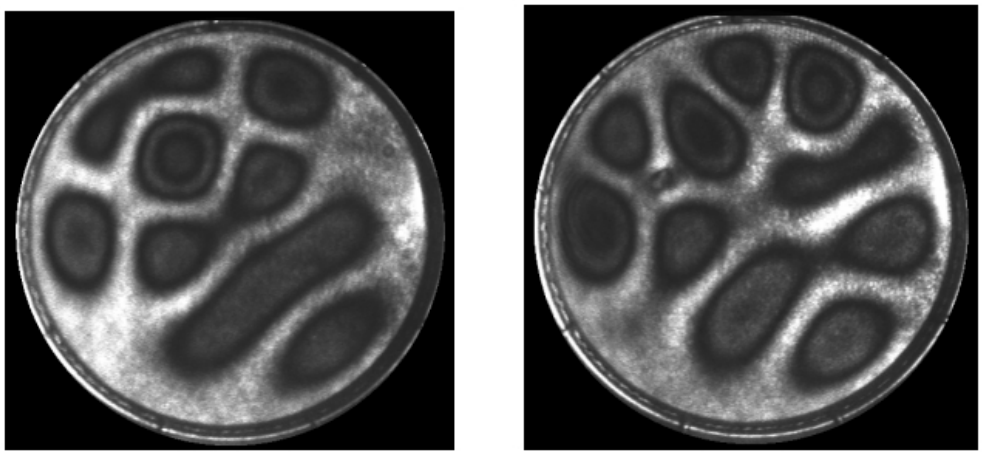

Figure 16 : The modal signature at 1820Hz for healthy and defected structures

5. Holographic interferometry with two reference beams

This technique allows for a digital calculation of micrometric displacements at each point of the surface of an object from its interferometric image. The principal of the method goes back to that for double exposition. By comparison with the classic set up of holographic interferometry by double exposition, there is simply the addition of a second reference beam which makes an acute angle with the first (figure 17) [10 [Interferometric Analysis by Wavefront Reconstruction],11 [Two-Reference-Beam Holographic Interferometry]]. The mirror 2 of the reference path 2 is mounted on a piezoelectric transducer which allows for the phase shift method to be applied during reconstruction [18 [Pulsed Digital Holography Combined With Laser Vibrometry for 3D Measurements of Vibrating Objects],19 [Phase Measurement Interferometry Techniques]].

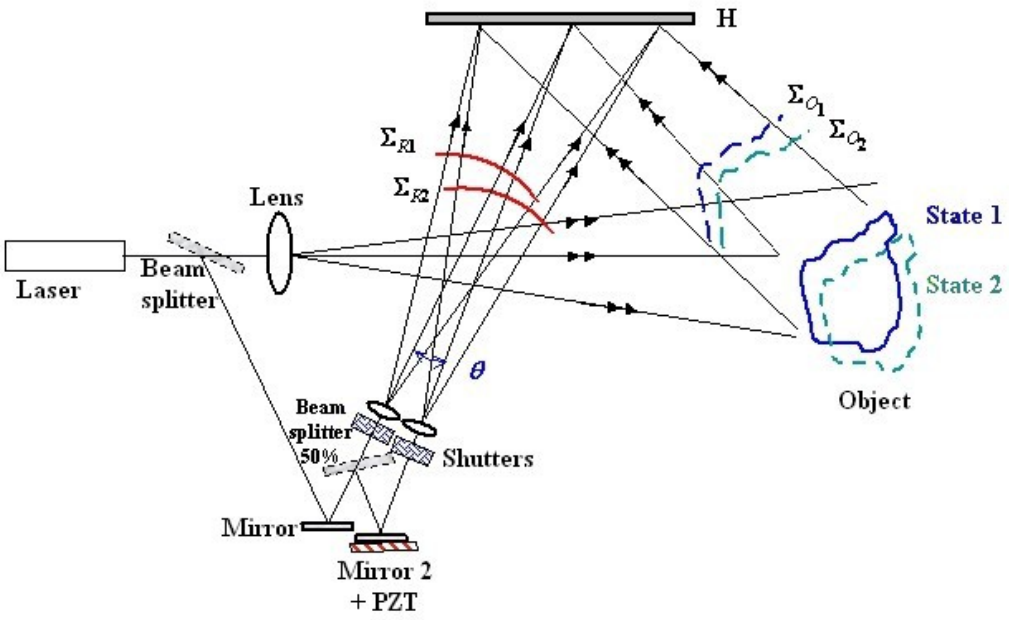

Fgure 17 : Holographic interferometry with two reference beams

The recording sequence is as follows :

- a first hologram is recorded with the first reference beam R_1 with the object in the first state ; the second reference beam R_2 is blocked by the shutter 2
- a second hologram is recorded with the reference beam $R_2$with the object in the second state ; the first reference beam R_1 is blocked by the shutter 1 ; the piezoelectric device is not active.

Two holograms of the object are obtained on the same photosensitive plate at two different instants and recorded with two different reference beams.

After the photosensitive plate is developed, the reconstruction by diffraction is carried out at the same time with the two beams R_1 and R_2 . Each reference beam gives its hologram corresponding to a holographic image. We therefore get two object beams in the $+1$-order which each correspond to a different state of the object. The two holographic images interfere with each other to give a fringe system which can be quantitatively analysed. Since the mirror 2 is mounted on a piezoelectric transducer, the relative optical phase of the two reference beams can be varied and techniques of demodulation by phase shift can be applied [18 [Pulsed Digital Holography Combined With Laser Vibrometry for 3D Measurements of Vibrating Objects],19 [Phase Measurement Interferometry Techniques]]. For example, by giving four values to the phase variation caused by the piezoelectric device, we get 4 interference equations which allow us to calculate the optic phase generated by the displacement of the object between two states. Thus, we can determine the amplitude and the displacement direction at each point of the object between the two states.

5.1. Theoretical Aspect

Let's note A_{R1} the complex amplitude of the reference wave R_1, $A_{R1} = a_1 \exp(j\varphi_1)$, and A_1 that of the object in state 1. We get

$$A_1(x,y) = A_0(x,y)\exp(j\psi_0(x,y))$$

Note also A_{R2} the complex amplitude of the reference wave R_2 in which we take into account the presence of the piezoelectric device which modulates the phase during the reconstruction ;

that is to say $A_{R2} = a_2\exp(j\varphi_2 + j\phi)$ with ϕ as the phase variation susceptible to being introduced by the phase shifter.
Also note A_2 the amplitude of the object in state 2. We get

$$A_2(x,y) \approx A_0(x,y)\exp(j\psi_0(x,y) + j\Delta\varphi(x,y))$$

At the recording, if Φ is null we get,

$$H = |R_1|^2 + |O_1|^2 + |R_2|^2 + |O_2|^2 + R_1 O_1^* + R_2 O_2^* + R_2^* O_2 + R_1^* O_1$$

The last two terms make up the $+1$-order

At the reconstruction with the first reference wave, the last term $-\beta\Delta t|R_1|^2 O_1$ corresponds to the $+1$-order. The same with the 2nd reference wave and the phase modulation caused by the piezoelectric device, when the third term $-\beta\Delta t|R_2|^2 O_2\exp(j\phi)$ corresponds to the $+1$-order.
We are only interested in the diffracted amplitude in the $+1$-order. The diffracted field in the $+1$ -order at the distance $-d_0$ from the plate, is given by the following for the first reference wave :

$$A_{R1}^{+1}(x,y,-d_0) = -\beta a_1^2 \Delta t\, A_0(x,y)\exp(j\psi_0(x,y)) * \widetilde{W}_A(x,y,-d_0)$$

And for the second reference wave we get

$$A_{R2}^{+1}(x,y,-d_0) = -\beta a_2^2 \Delta t\, A_0(x,y)\exp(j\psi_0(x,y))\exp(j\Delta\varphi(x,y) + j\phi) * \widetilde{W}_A(x,y,-d_0)$$

The image seen by the observer is linked to the squared modulus of the diffracted field. By omitting the enlargement function, we get

$$\begin{aligned} I_R^{+1}(x,y,-d_0) &= |A_{R1}^{+1}(x,y,-d_0) + A_{R2}^{+1}(x,y,-d_0)|^2 \\ &= \beta^2 \Delta t^2 A_0^2(x,y)\left(a_1^2 + a_2^2 + 2a_1 a_2 \cos(\Delta\varphi(x,y) + \phi)\right) \end{aligned}$$

It is an expression in the form

$$I_R^{+1} = E = a + b\cos(\Delta\varphi + \phi)$$

The image in the $+1$-order is therefore modulated by a fringe network linked to the optical phase variation generated by the displacement of the object between two states.
If we give 4 discreet values to the phase shift such as $\phi = (n-1)\pi/2$, $n = 1,2,3,4$ we get 4 dephased interferograms in the $+1$-order.

$$E_1 = a + b\cos(\Delta\varphi)$$

$$E_2 = a + b\cos(\Delta\varphi + \pi/2)$$

$$E_3 = a + b\cos(\Delta\varphi + \pi)$$

$$E_4 = a + b\cos(\Delta\varphi + 3\pi/2)$$

The phase $\Delta\varphi$ can be digitally calculated modulo 2π by

$$\Delta\varphi = \arctan\left(\frac{E_4 - E_2}{E_1 - E_3}\right)$$

The amplitude of the oscillation of the fringes can be evaluated by :

$$b = \frac{1}{2}\sqrt{(E_1 - E_3)^2 + (E_4 - E_2)^2}$$

And the offset is determined by :

$$a = \frac{1}{4}(E_1 + E_2 + E_3 + E_4)$$

Thus, the modulation rate of the fringes can be determined :

$$m = \frac{b}{a} = \frac{2\sqrt{(E_1 - E_3)^2 + (E_4 - E_2)^2}}{E_1 + E_2 + E_3 + E_4}$$

The measurement of the modulation rate can be used to discern the pixels of the image which must be processed from those which must not. It is possible, for example, to fix a minimum threshold for this parameter above which it is considered that the pixel has been sufficiently modulated that the phase measurement has some significance.

5.2. The limitations of this procedure

The device is delicate to set up which can limit its uses.

5.3. The experimental set-up

The set-up for the reconstruction of holograms is shown in figure 18. The hologram is illuminated by two reference beams at the same time.

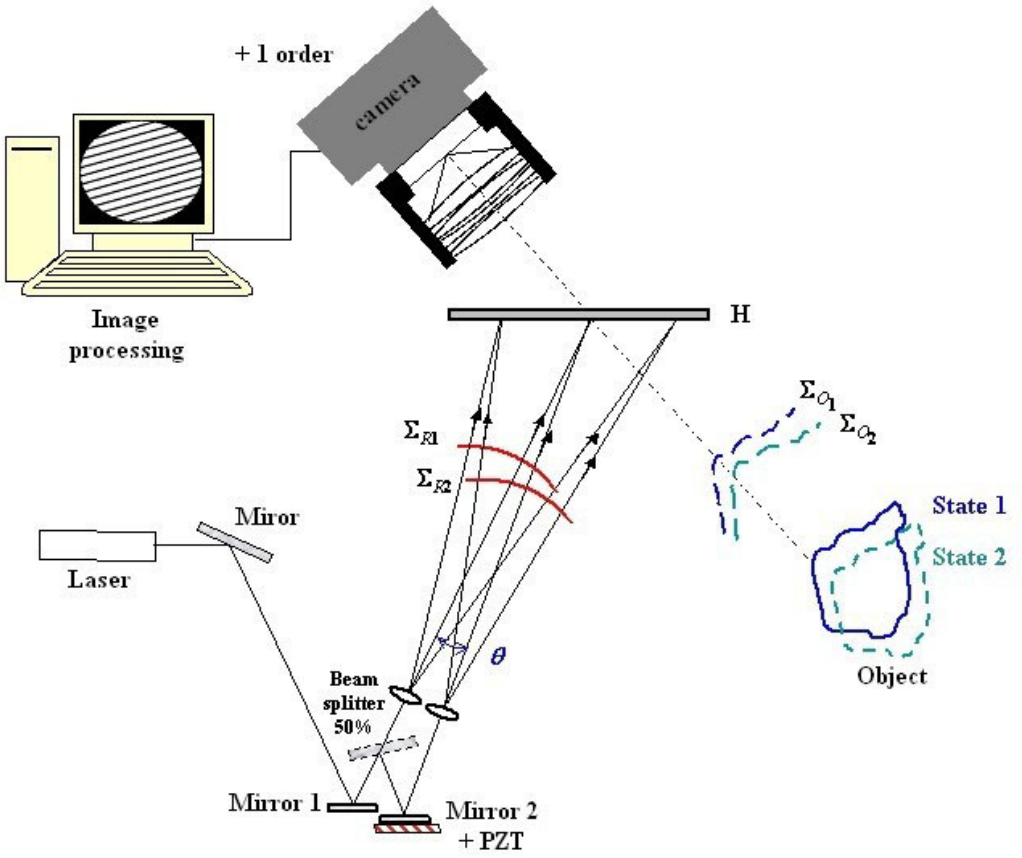

Figure 18 : Reconstruction with two reference beams

The camera records the interferograms after the introduction of the phase shift with the piezoelectric transducer.

5.4. Applications and uses

This method can be used with a continuous or pulsed laser for the quantification of defects in non-destructive testing and in the analysis of vibrations in the automobile or aeronautic industries for example.

5.5. Illustration

Figure 19 presents 4 interferograms dephased by $\pi/2$ obtained during the testing of the adhesiveness of a structure made of several materials. The illustration of the fringes shows a defect located at the centre of the image.

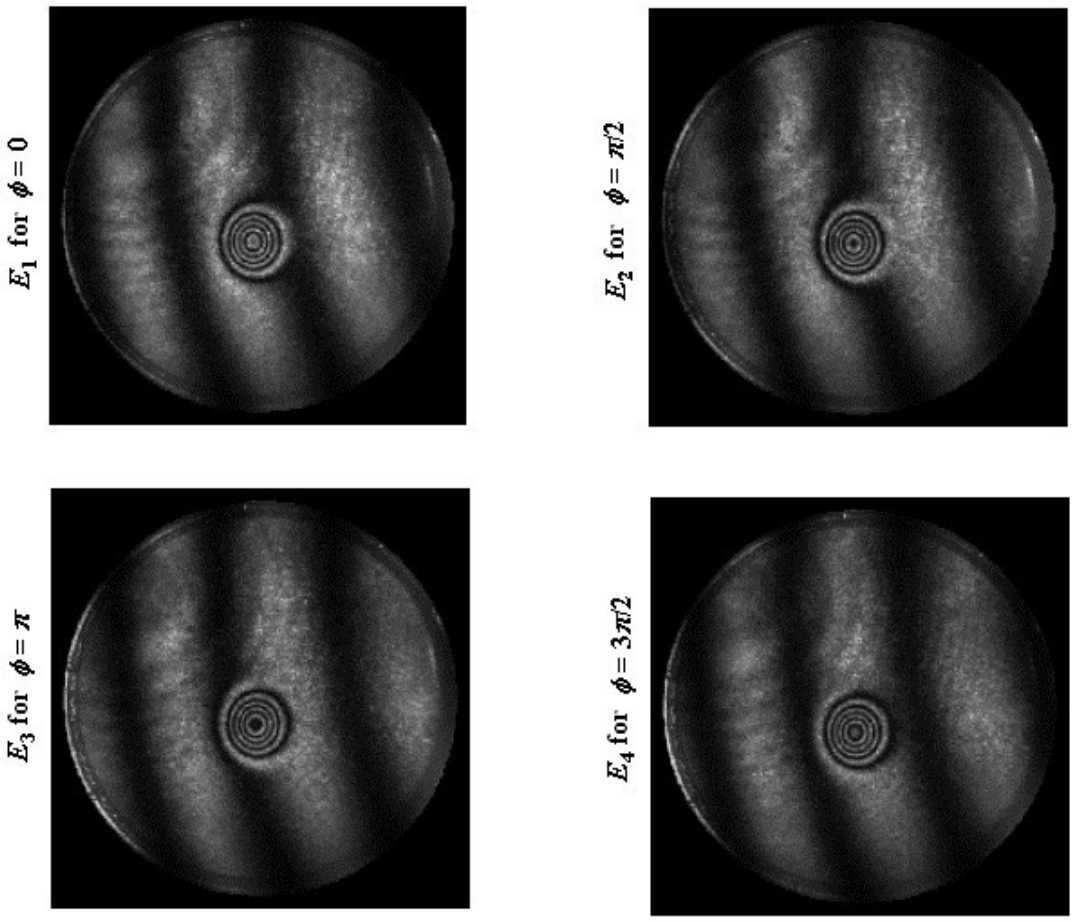

Figure 19 : dephased interferograms

Figure 20 shows the phase variation calculated modulo 2π with the 4 interferograms.

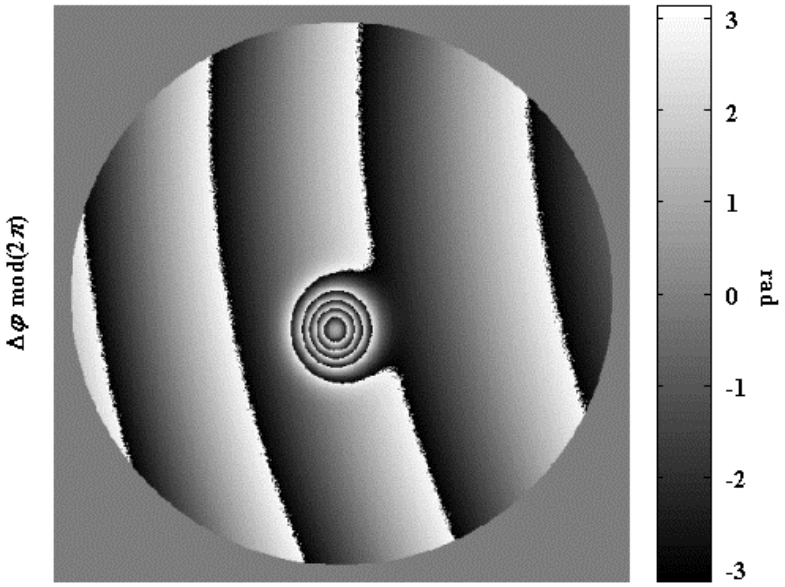

Figure 20 : Phase variation calculated modulo 2 π

Figure 21 shows the phase variation after the processing of its 2π-discontinuities by a specific algorithm.

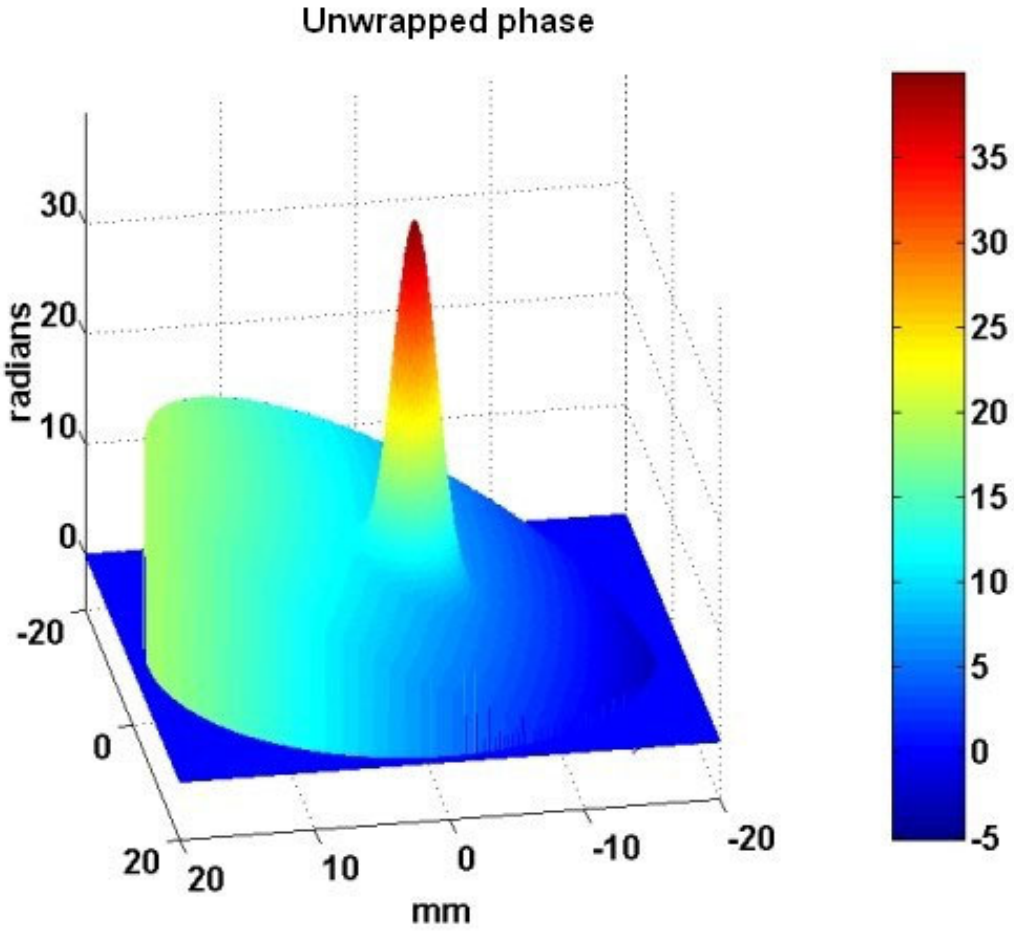

Figure 21 : Phase variation uncoiled

6. Digital holographic interferometry with time averaging

The principle of this technique is identical to that of analogue holography with time averaging: the hologram of the object in vibration is recorded with an exposure time Δt which is longer than the vibration period. However, the hologram is recorded with a matrix of photo-detectors and the diffracted field is digitally reconstructed by calculating a discreet Fresnel transform [12 [Fringe Interpolation by Two-Reference-Beam Holographic Interferometry : Reducing Sensitivity to Hologram Misalignment],13 [Time-Averaged Digital Holography],14 [Some Opportunities for Vibration Analysis with Time-Averaging in Digital Fresnel Holography],15 [Dynamic Modal Characterization of Musical Instruments Using Digital Holography]].

6.1. Theoretical Aspect

By looking again at the theoretical analysis proposed in the paragraph which dealt with analogue holography with time averaging, and by considering the fact that the recording and reconstruction are discretised, the digitally diffracted field in the $+1$-order is given by :

$$A_R^{+1}(x,y,-d_0)=\lambda^2 d_0^2 \exp\left(-j\pi\lambda d_0\left(u_R^2+v_R^2\right)\right) R^*(x,y)\ A(x,y)$$
$$\times\int_{t_1}^{t_1+\Delta t}\exp\left(j\Delta\varphi_0(x,y)\sin(\omega_0 t+\varphi_0(x,y))\right)\ dt$$
$$*\widetilde{W}_{NM}(x,y,-d_0)*\delta(x-\lambda d_0 u_R, y-\lambda d_0 v_R)$$

Being also

$$A_R^{+1}(x,y,-d_0)=\Delta t\,\lambda^2 d_0^2 \exp\left(-j\pi\lambda d_0\left(u_R^2+v_R^2\right)\right) R^*(x,y)\ A(x,y)\ J_0(\Delta\varphi_0(x,y))$$
$$*\widetilde{W}_{NM}(x,y,-d_0)*\delta(x-\lambda d_0 u_R, y-\lambda d_0 v_R)$$

Since

$$J_0(\Delta\varphi_0(x,y))=|J_0(\Delta\varphi_0(x,y))|\exp\left(j\varphi_J(x,y)\right)$$

The optical phase in the digital $+1$-order is written :

$$\arg\left(A_R^{+1}(x,y,-d_0)\right)=-\pi\lambda d_0\left(u_R^2+v_R^2\right)-2\pi(u_R x+v_R y)$$
$$+\psi_0(x,y)+\varphi_J(x,y)$$

The terms which make up the digital phase are in part linked to the spatial frequencies of the reference wave and correspond to an inclined phase plane; they are invariant in time whatever the method used to record the hologram (with averaging or without). The same goes for the random-speckle phase $\psi_0(x,y)$. These terms are without great interest given that in digital holography it is often necessary to resort to phase subtraction and these terms would not come into the equation.

It can be stated that the information on the phase of the mechanical vibration $\varphi_0(x,y)$is not contained in the calculated object field. Thus, the technique of digital time averaging only gives information on the amplitude of object displacements. The term $\varphi_J(x,y)$ introduced in the phase equation is defined as follows [13 [Time-Averaged Digital Holography]] :

$$\varphi_J(x,y)=\begin{pmatrix}0 \text{ if } J_0(\Delta\varphi_0)>0\\ \pi \text{ if } J_0(\Delta\varphi_0)<0\end{pmatrix}$$

The phase $\varphi_J$is a binary variable which takes the value 0 or π. Its transitions between these values pinpoint the phase skip at which time the Bessel function J_0 passes through 0. The phase $\varphi_J$therefore corresponds to the phase of the Bessel function passing through 0 (“zero-crossing”), Thus, in the case where the object is recorded in stasis, without sinusoidal stimulation, the phase of the reconstructed object is given by

$$\psi_{stat}=-\pi\lambda d_0\left(u_R^2+v_R^2\right)-2\pi(u_R x+v_R y)+\psi_0(x,y)$$

When the same object is reconstructed after recording with time averaging, its phase becomes

$$\psi_{moy} = -\pi \lambda d_0 \left(u_R^2 + v_R^2 \right) - 2\pi \left(u_R x + v_R y \right) + \psi_0(x, y) + \varphi_J(x, y)$$

The phase of "zero-crossing" is therefore directly extracted from the phase difference, that is to say

$$\varphi_J = \psi_{moy} - \psi_{stat}$$

Given the binary character of φ_J, the determination of the phase jumps of this last equation allows for a precise determination of the contour lines associated with the Bessel function passing through 0. This method gives a strong contrast to the rate of passages though 0.

The reader should note that this property is unique to digital holography which gives direct access to the optical phase during the calculation of the diffracted field. Indeed, in analogue holography with time averaging, it is only possible to observe the squared modulus of the Bessel function, its phase is therefore intrinsically lost.

6.2. The limitations of this procedure

The principal limitation of this method is its low resolution character since the recording is carried out with a pixel matrix which is only several microns in size. However, its big advantage is that there are no consumables and that the digital treatment of images can be developed in an extreme manner in order to increase the quality of reconstructions.

6.3. The experimental set-up

The experimental set-up for the recording of a digital hologram is a Mach-Zehnder-type interferometer (figure 22). The laser beam is separated into two beams by a cube. For a complete description, the reader should turn to the case study section of the course entitled "recording/reconstruction."

The sensor exposure time must be adjusted taking in to account the incident flux (object and reference) and the stimulation period because the condition $\Delta t > 2\pi/\omega_0$ must be respected.

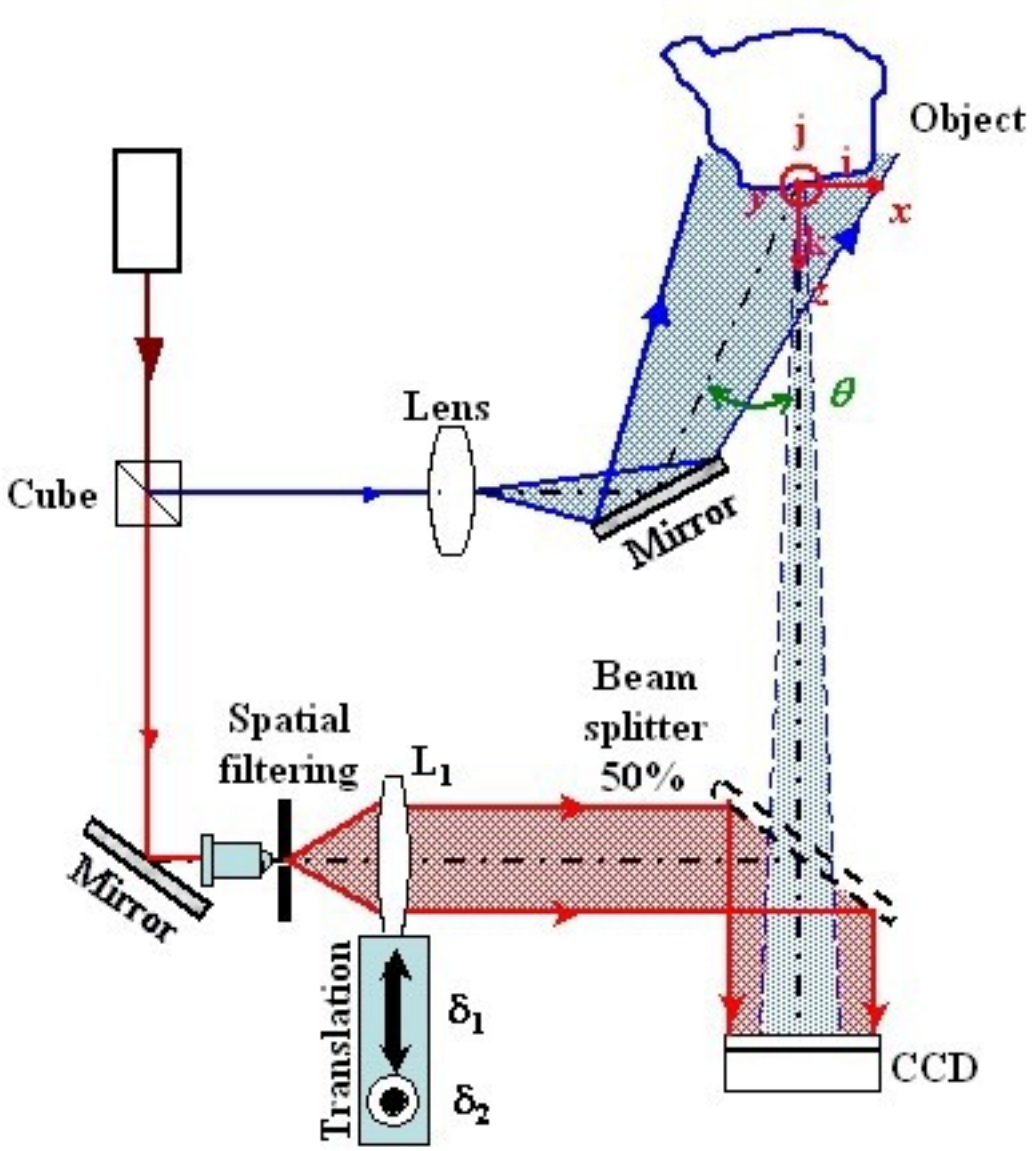

Figure 22 : Digital holographic interferometer

6.4. Applications and uses

The field of applications for this technique centres on the vibration analysis of small objects because of the limited resolution, by comparison with analogue holography which is very well adapted to larger structures.

6.5. Illustration

As an illustration, let's consider a loud speaker, $60\ \text{mm}$ in diameter placed at a distance $d_0 = 1385\ \text{mm}$ from the sensor. The exposure time of the image sensor is $\Delta t = 1\ \text{s}$. The source which is used is a He-Ne laser. The spatial frequencies of the carrier wave are adjusted to $u_R = 69\ \text{mm}^{-1}$ and $v_R = 72.2\ \text{mm}^{-1}$. The reconstruction is calculated over 2048 points with zero-padding. The illumination angle of the object is $\theta = 35$. Figure 23 illustrates the field calculated by the discreet Fresnel transform of the hologram with time averaging. The reconstruction of the $+1$-order shows the Bessel modulation. The frequency of the stimulation of the loud speaker is $3700\ \text{Hz}$.

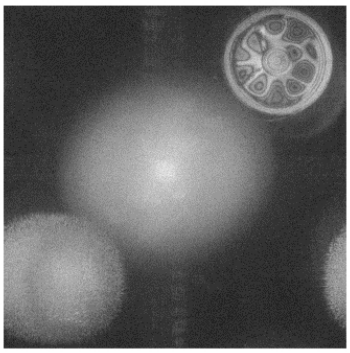

Figure 23 : The reconstructed field emanating from the digital hologram with time averaging

Figure 24 represents the $+1$-order which is obtained for three different sinusoidal stimulation amplitudes (respectively weak, medium and high). The amplitude modulation is clearly visible on the reconstructed loud speaker. The dark fringes are densely packed for the medium and strong amplitude levels and it becomes more difficult to distinguish them in certain areas.

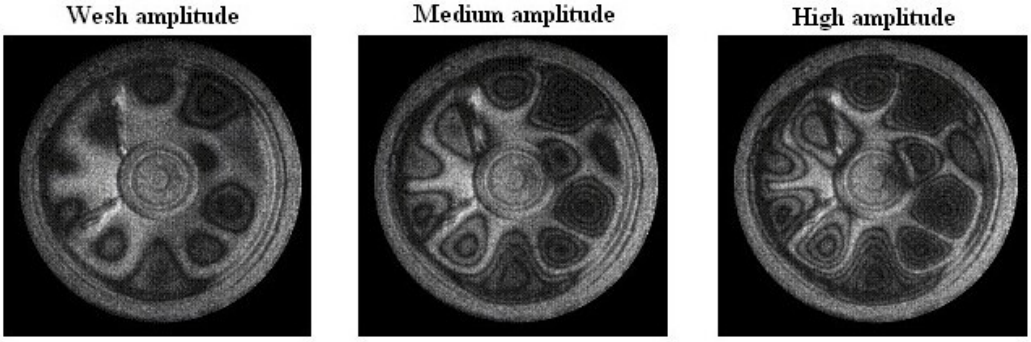

Figure 24 : Time averaging method applied to the loud speaker with a simulation frequency of 3700Hz for different vibration amplitudes

The zero-crossing phase can be calculated from the acquisition of the two digital holograms, the first when the object is static and the second by time averaging. Figure 25 shows the zero-crossing phase extracted by subtraction of the object phases in the static state and by time averaging and the phases for the three stimulation amplitudes. The phase $\varphi_J$is characterised by zones of constant phase and zones of phase jump. As predicted, this phase pinpoints (with light contrast) the phase jumps for $\varphi_J$which match perfectly with the location of the dark fringes represented in figure 23. the phase jumps are very easily discernible compared to the dark fringes.

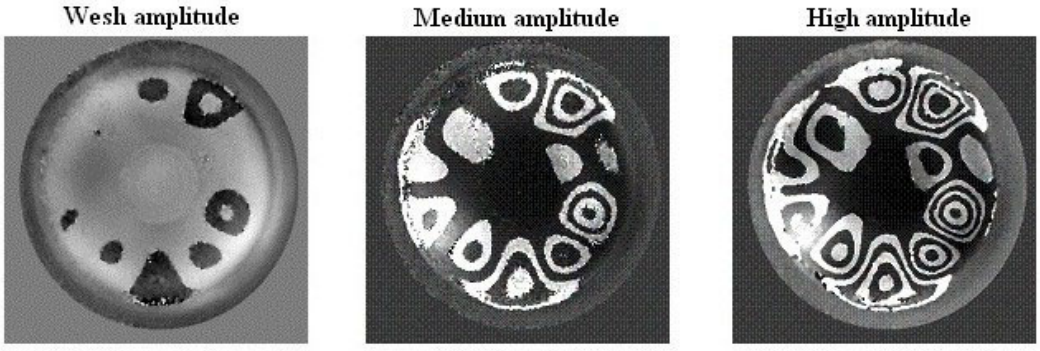

Figure 25 : Phase for the zero-crossing of the loud speaker stimulated at 3700Hz for different vibration amplitudes

Determining phase jumps for $\varphi_J$is an excellent way of precisely determining the contour lines associated with the passing through 0 of the Bessel function. The zeros are linked to the vibration amplitude and the sensitivity vector of the recording device. Since the loud speaker essentially vibrates according to an out of plane component, the vector for the vibration of the object is $\mathbf{U}(t) = u_z \sin(\omega_0 t + \varphi_0)\mathbf{k}$ and the sensitivity vector is $\mathbf{S} = (1 + \cos\theta)\mathbf{k}$ on the Cartesian reference frame attached to the object (figure 22). The reader should verify that for each zero of the modulation, the vibration amplitude is expressed by :

$$u_z(x,y) = \frac{\lambda}{2\pi} \frac{1}{1+\cos\theta}\, \omega_n(x,y)$$

Figure 26 shows the contour lines extracted from the detection of phase contours on figure 25. These lines are interpreted as lines of displacement-level amplitude. The displacement amplitudes corresponding to the nth passage though 0 are given in table 2.

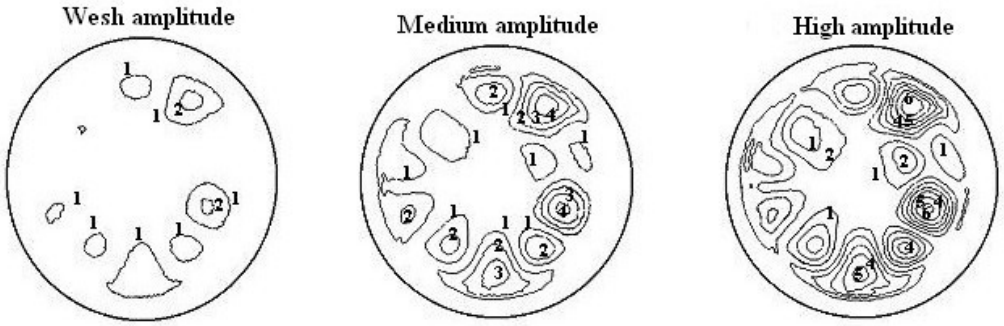

Figure 26 : Contour lines corresponding to the nth passage through 0

n	ω_n(rad)	u_z (µm)
1	2.4	0.13
2	5.52	0.3
3	8.65	0.47
4	11.79	0.64
5	14.93	0.81
6	18.07	0.99

Table 2 : Correspondence between the number of passages through 0 and the displacement amplitude for an observation angle of 35°

The passages through 0 are numbered 1 to 6 on the contour lines shown in figure 25. The reader should note that the raised amplitude contour lines from figure 25 cannot be easily extracted from the image directly calculated in the $+1$-order which is represented in figure 23, because of the weak contrast. However, this problem is resolved by considering the phase of the passages through 0 of the Bessel function and this shows the interest in this technique when the fringes are tightly packed.

6.6. Digital/Analogue comparison

Figure 27 shows images of the reconstruction of the loud speaker by analogue holography so that the reader can better appreciate the similarities and differences between the digital and analogue methods of reconstruction with time averaging; images of the digital reconstruction in the $+1$-order are also shown. Note the correlation between the analogue and digital fringes. However, the difference in resolution between analogue and digital holography is remarkable. The anaogic recording plate is made up of dichromatic gelatine with a resolution of $5000\ \mathrm{mm}^{-1}$

with grains of $15\ \text{nm}$ for a sensitivity of $85\ \mu\text{J/cm}^2$. The plate dimensions are $10.16 \times 12.7\ \text{cm}^2$. The resolution is therefore up to 20 times better (in the largest dimension) with analogue holography. The conditions for illuminating the object are identical to those for the digital holographic device. The slight differences between the image of the fringes comes from the hygrometry and the temperature which are not totally identical during the digital and analogue recordings.

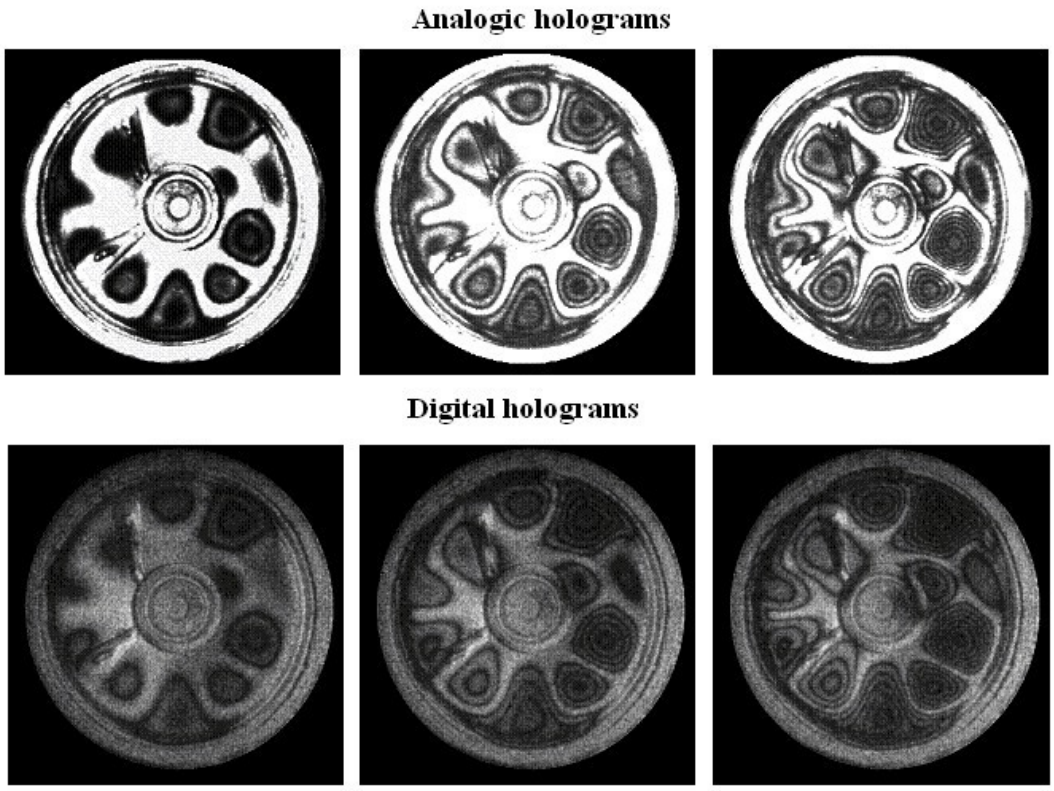

Figure 27 : Comparison between analogue and digital time averaging for different vibration amplitudes of a loud speaker stimulated at 3700Hz

The images obtained by classical holography correspond to the squared modulus of the diffracted field in the $+1$-order, which is not the case in digital holography given that the calculation gives access to the complex image. That is why, the extraction of the zero-crossing phase is impossible in analogue holography, but it is compensated by a noticeably better resolution.

7. Digital holographic vibrometry

It should be noted that holography with time averaging does not give any information on the mechanical phase $\varphi_0(x,y)$, that is to say that we don't have the capacity to simply find out the relative direction of the displacements between two vibrating zones, since the temporal integration excludes the information on the signal of the displacement amplitude. This paragraph introduces digital holographic vibrating which allows the amplitude and the vibration phase to be reconstructed [16 [Time-Averaged In-Line Digital Holographic Interferometry for Vibration Analysis],17 [Full Field Vibrometry With Digital Fresnel Holography]].

7.1. The theoretical aspect

The reconstruction of a vibration by amplitude and phase requires the processing of the optical phase of a digital hologram. Indeed, let's take the expression of the reconstructed object in the case of the time averaging method. We have seen that its expression is given by

$$A_R^{+1}(x,y,-d_0)=\lambda^2 d_0^2 \exp\left(-j\pi\lambda d_0\left(u_R^2+v_R^2\right)\right) R^*(x,y)\ A(x,y)$$
$$\times\int_{t_1}^{t_1+\Delta t}\exp\left(j\Delta\varphi_0(x,y)\sin\left(\omega_0 t+\varphi_0(x,y)\right)\right)\ dt$$
$$*\widetilde{W}_{N\,M}(x,y,-d_0)*\delta\left(x-\lambda d_0 u_R, y-\lambda d_0 v_R\right)$$

From now on, let's consider that the exposure time or the duration of the illumination is a lot smaller than the vibration period, which is to say that we get

$$\frac{\Delta t}{T_0}<\frac{1}{\Delta\varphi_0}$$

The justification of this inequality will not be tackled in this booklet. For extra information, the reader should consult the reference section [[Time-Averaged In-Line Digital Holographic Interferometry for Vibration Analysis]]. In these recording conditions we get

$$\int_{t_1}^{t_1+\Delta t}\exp\left(j\Delta\varphi_0\sin\left(\omega_0 t+\varphi_0\right)\right)dt=\Delta t\exp\left(j\Delta\varphi_0\sin\left(\omega_0 t_1+\varphi_0\right)\right)$$

Thus, the phase which is extracted from each hologram at each moment of the recording t_n encodes the amplitude and vibratory phase according to the expression :

$$\arg\left(A_R^{+1}(x,y,-d_0,t_n)\right)=-\pi\lambda d_0\left(u_R^2+v_R^2\right)-2\pi(u_R x+v_R y)$$
$$+\psi_0(x,y)+\Delta\varphi_0(x,y)\sin\left(\omega_0 t_n+\varphi_0(x,y)\right)$$

We will keep the following expression, which gets rid of the unimportant terms :

$$\psi_n=\psi_0+\Delta\varphi_0\sin\left(\omega_0 t_n+\varphi_0\right)$$

This equation contains 3 unknowns $\{\psi_0,\Delta\varphi_0,\varphi_0\}$ in which two are linked to the studied vibration. At least 3 equations are necessary to resolve it. The normal method consists in recording at least 3 digital holograms with phaseshift relative to the stimulation. It is noted that the number of holograms can be increased in order to over-determine the system and to bring more robustness to the estimation of the 3 unknowns. The reader will remark that this method would be extremely difficult to put into place with an analogic holographic bench because it would be necessary to develop a structure with two reference beams. Digital holography is thus the best candidate for full field vibrometry even if the final analysis must lose out in terms of spatial resolution.

Let's consider the recording of a number of holographic pairs dephased in relation to the stimulation; 8 pairs for example: The 8 phases of the holograms encode the following information :

$$\psi_n=\psi_0+\Delta\varphi_0\sin\left(\omega_0 t_0+\varphi_0+\phi_n\right)\quad \mathrm{mod}(2\pi)\quad n\in[1,8]$$

Where we would choose $\phi_n=(n-1)2\pi/8$ and where t_0 is the instant at which the recording begins. Let's develop the expression under the form

$$\psi_n = \psi_0 + \Delta\varphi_0 \sin(\omega_0 t_0 + \varphi_0)\cos(\phi_n) + \Delta\varphi_0 \cos(\omega_0 t_0 + \varphi_0)\sin(\phi_n)$$

Phase differences can be formed :

$$\begin{aligned}\Delta\Psi_1 = \psi_1 - \psi_5 = {} & \Delta\varphi_0 \sin(\omega_0 t_0 + \varphi_0)[\cos(\phi_1) - \cos(\phi_5)] \\ & + \Delta\varphi_0 \cos(\omega_0 t_0 + \varphi_0)[\sin(\phi_1) - \sin(\phi_5)]\end{aligned}$$

$$\begin{aligned}\Delta\Psi_2 = \psi_2 - \psi_6 = {} & \Delta\varphi_0 \sin(\omega_0 t_0 + \varphi_0)[\cos(\phi_2) - \cos(\phi_6)] \\ & + \Delta\varphi_0 \cos(\omega_0 t_0 + \varphi_0)[\sin(\phi_2) - \sin(\phi_6)]\end{aligned}$$

$$\begin{aligned}\Delta\Psi_3 = \psi_3 - \psi_7 = {} & \Delta\varphi_0 \sin(\omega_0 t_0 + \varphi_0)[\cos(\phi_3) - \cos(\phi_7)] \\ & + \Delta\varphi_0 \cos(\omega_0 t_0 + \varphi_0)[\sin(\phi_3) - \sin(\phi_7)]\end{aligned}$$

$$\begin{aligned}\Delta\Psi_4 = \psi_4 - \psi_8 = {} & \Delta\varphi_0 \sin(\omega_0 t_0 + \varphi_0)[\cos(\phi_4) - \cos(\phi_8)] \\ & + \Delta\varphi_0 \cos(\omega_0 t_0 + \varphi_0)[\sin(\phi_4) - \sin(\phi_8)]\end{aligned}$$

The differences are estimated $\mod(2\pi)$ and it is therefore necessary to uncoil the phase in order to extract the mechanical amplitude and phase. After the phase is uncoiled, the differences are expressed in the form:

$$\Delta\Psi_i = a_i \Delta\varphi_0 \sin(\omega_0 t_0 + \varphi_0) + b_i \Delta\varphi_0 \cos(\omega_0 t_0 + \varphi_0) \quad i \in [1,4]$$

Thus also

$$\Delta\Psi_i = a_i \alpha + b_i \beta$$

with

$$\begin{aligned}\alpha &= \Delta\varphi_0 \sin(\omega_0 t_0 + \varphi_0) \\ \beta &= \Delta\varphi_0 \cos(\omega_0 t_0 + \varphi_0)\end{aligned}$$

$$a_1 = \cos(\phi_1) - \cos(\phi_5) \qquad b_1 = \sin(\phi_1) - \sin(\phi_5)$$

$$a_2 = \cos(\phi_2) - \cos(\phi_6) \qquad b_2 = \sin(\phi_2) - \sin(\phi_6)$$

$$a_3 = \cos(\phi_3) - \cos(\phi_7) \qquad b_2 = \sin(\phi_3) - \sin(\phi_7)$$

$$a_4 = \cos(\phi_4) - \cos(\phi_8) \qquad b_2 = \sin(\phi_4) - \sin(\phi_8)$$

Regarding the least squares sens, the data $\Delta\Phi_i$ should minimise the following proximity criteria :

$$\epsilon = \sum_{i=1}^{i=4} [\Delta\Psi_i - a_i\alpha - b_i\beta]^2$$

Of which the derivatives should be null :

$$\frac{\partial\varepsilon}{\partial\alpha} = \frac{\partial\varepsilon}{\partial\beta} = 0$$

This leads to a linear system of 2 equations to 2 unknowns. We get :

$$\sum_{i=1}^{i=4} a_i^2\alpha + a_i b_i\beta = \sum_{i=1}^{i=4} a_i\Delta\Psi_i$$
$$\sum_{i=1}^{i=4} a_i b_i\alpha + b_i^2\beta = \sum_{i=1}^{i=4} b_i\Delta\Psi_i$$

thus also

$$A(a_i, b_i)X = B(\Delta\Psi_i, a_i, b_i)$$

where

$$A(a_i, b_i) = \begin{pmatrix} \sum_{i=1}^{i=4} a_i^2 & \sum_{i=1}^{i=4} a_i b_i \\ \sum_{i=1}^{i=4} a_i b_i & \sum_{i=1}^{i=4} b_i^2 \end{pmatrix}$$

$$X = \begin{pmatrix} \alpha \\ \beta \end{pmatrix}$$

$$B(\Delta\Psi_i, a_i, b_i) = \begin{pmatrix} \sum_{i=1}^{i=4} a_i\Delta\Psi_i \\ \sum_{i=1}^{i=4} b_i\Delta\Psi_i \end{pmatrix}$$

The inversion gives

$$X = A^{-1}(a_i, b_i)B(\Delta\Psi_i, a_i, b_i)$$

The matrix $A^{-1}(a_i, b_i)$ can be digitally estimated from the knowledge of the delays $\Delta T_n = \phi_n/\omega_0 = (n-1)/8f_0$ for each recording. The amplitude of the mechanical vibration is calculated with the relationship

$$\Delta\varphi_0=\sqrt{\alpha^2+\beta^2}$$

And the phase of the mechanical vibration is estimated by

$$\varphi_0=\arctan\left(\frac{\alpha}{\beta}\right)-\omega_0 t_0$$

The reader should note that the term $\omega_0 t_0$is only a constant to be removed and that it is physically meaningless since calculation by arctangent always results in being to the nearest constant. This term can thus be left out of the calculation.

7.2. The limitations of this procedure

The method will work if the following conditions can be assured : $\Delta t < 1/f_0\Delta\varphi_0$. For example, if the vibration amplitude is such that the corresponding optical phase is $\Delta\varphi_0 = 20\ \text{rad}$ for a frequency of $f_0 = 5000\ \text{Hz}$ then it is necessary that $\Delta t < 10\ \mu\text{s}$. It is therefore necessary to use a pulsed laser source. Another constraint comes from the need to record holograms which are dephased by comparison to the stimulation. The experimental device should be conceived so that it permits different electro-optic elements (laser, sensor, object stimulation) to be synchronised.

7.3. The experimental device

A typical experimental device is shown in figure 28.

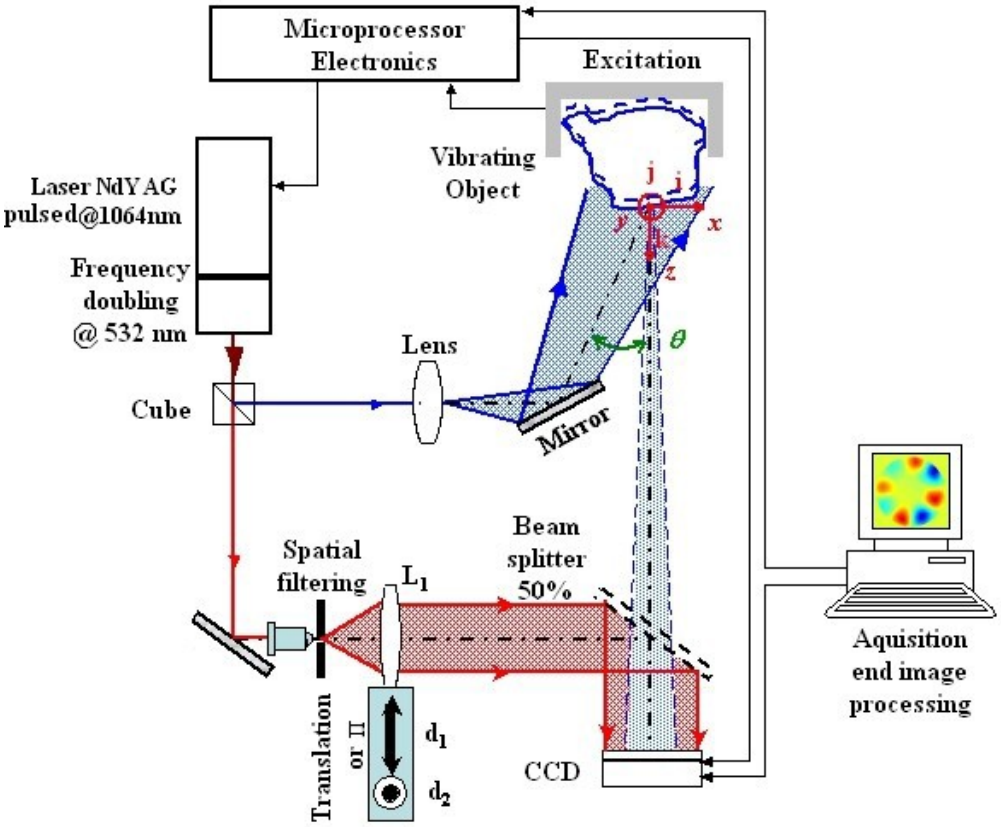

Figure 28 : Full field digital holographic vibrometer

The laser is a Nd:YAG, which is pulsed and doubled. The duration of the pulses coming from the laser is in the order of $20\,\mathrm{ns}$, their wave lengths at $532\,\mathrm{nm}$ and their energy can reach $500\,\mathrm{mJ}$. The midpoint of the laser is an Nd:YAG bar constituted by a matrix of YAG doped with neodyme ions. The pumping of the bar is assured by a flash lamp, circled by a diffuser so as to optimise the population inversion. The laser is set off by a cell of intracavity Packels. This module serves as an optical light switch. When the Pockel cell is set off, it acts as a quarter-wave plate thus authorising the laser's amplification process by return trip of the laser wave trains between the two mirrors of the cavity. The Pockel cell is generally switched on by applying a tension of $3\,\mathrm{kV}$. The pulses are emitted at a wave length of $1064\,\mathrm{nm}$ then their optic frequency is doubled by a KDP crystal placed at the exit of the cavity, thus they are emitted as impulsion trains of wave length $532\,\mathrm{nm}$. The setting off of the laser is driven by :

- the setting off of the flash lamp; generally the cadence of the flash lamp cannot exceed $60\,\mathrm{Hzz}$ and it can be of several Hz values which depends on the energy supplied by the laser,
- the control of the Pockel cell; the Pockel cell is linked to a high tension switch, which applies a high tension to the cell terminals when set off by an electric impulse,
- the Pockel cell must commute with a delay determined in relation with the pulsing signal of the flash lamp.

The device for controlling the laser uses a sensor placed on the object (microphone or accelerometer) or even a reference signal supplied by the stimulation system. Thus, we have an electric signal which is representative of the object's vibration and which serves to generate the phaseshifted holograms.

The acquisition technique is based on the stroboscopic principle ; the reference instant having been chosen, the laser impulse is brought forward by $n\Delta T + k'/f_0$. The integer coefficient k' indicates the number of oscillation periods before the next laser pulse and the integer coefficient n gives the time increment between the nth laser pulse and the first laser pulse. Thus, it is possible to finely sweep a period of object's oscillation by a temporal pitch ΔT by carrying out incremented laser pulses of a time lag ΔT relative to the vibration over different periods of stimulation. Figure 29 represents the principal of the stroboscopic laser pulse.

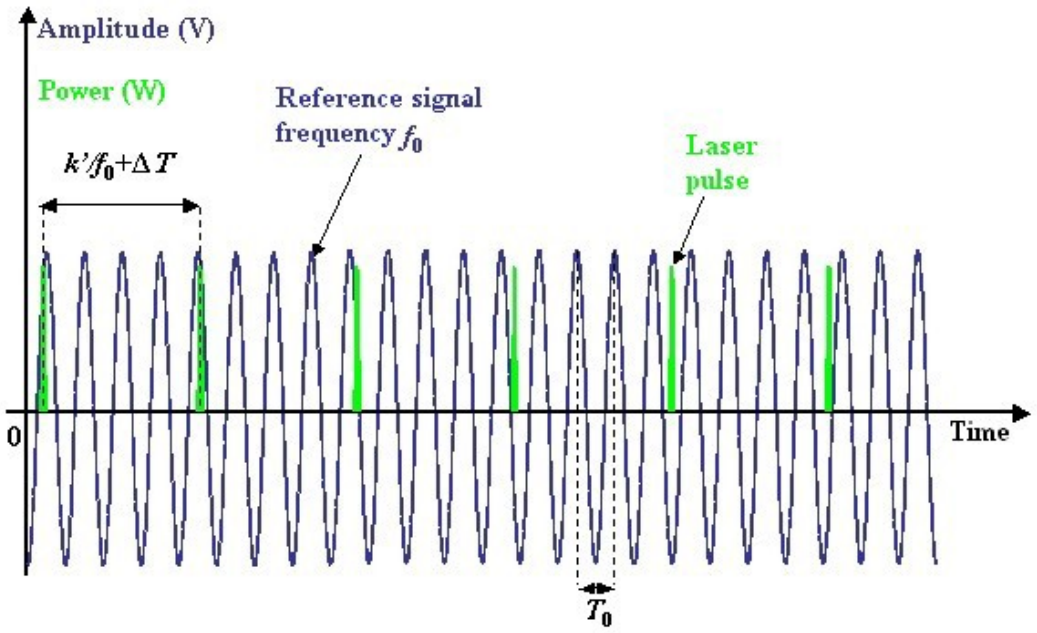

Figure 29 : Principal of the stroboscopic

The coefficient k' depends on the acquisition parameters :

- the maximum operating frequency of the CCD camera

- the frequential range of the triggering of the laser pulsing
- the fundamental frequency of the object stimulation (f_0)
- the temporal increment ΔT.

The control of the laser can be set via a grafical interface which allows for the laser impulse sequences to be programmed.

7.4. Applications and uses

This method is dedicated to the analysis of vibrations of any sort of objects, either in a forced oscillation system where the laser drives the stimulation or in an auto-oscillation regim where it is the signal issued from the object which drives the laser and the acquisition process.

7.5. Illustrations

The method is illustrated in the case study through the vibration behaviour of a clarinet reed in a forced oscillation regim. The reed is stimulated by a loud speaker which provides a reference signal which serves to drive the laser and the acquisition of the holograms. The process is applied with 8 holograms for frequencies $f_0 = 5400\ \mathrm{Hz}$ and $f_0 = 6000\ \mathrm{Hz}$. Figure 30 shows the 4 phase differences $\Delta\psi_i \bmod 2\pi$ obtained by subtraction of the raw phases of the 8 holograms for $f_0 = 5400\ \mathrm{Hz}$. Figure 31 shows the unwrapped phases, figure 32 and 33 show the amplitude and the vibration phase calculated from these results.

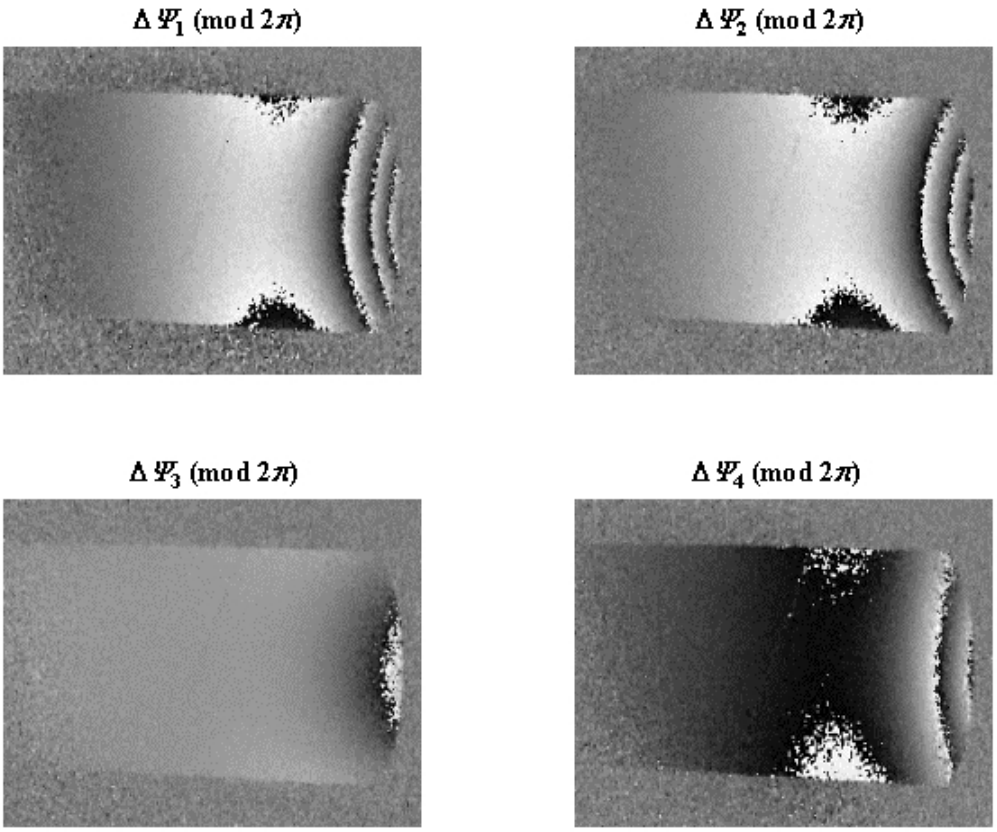

Figure 30 : phase differences

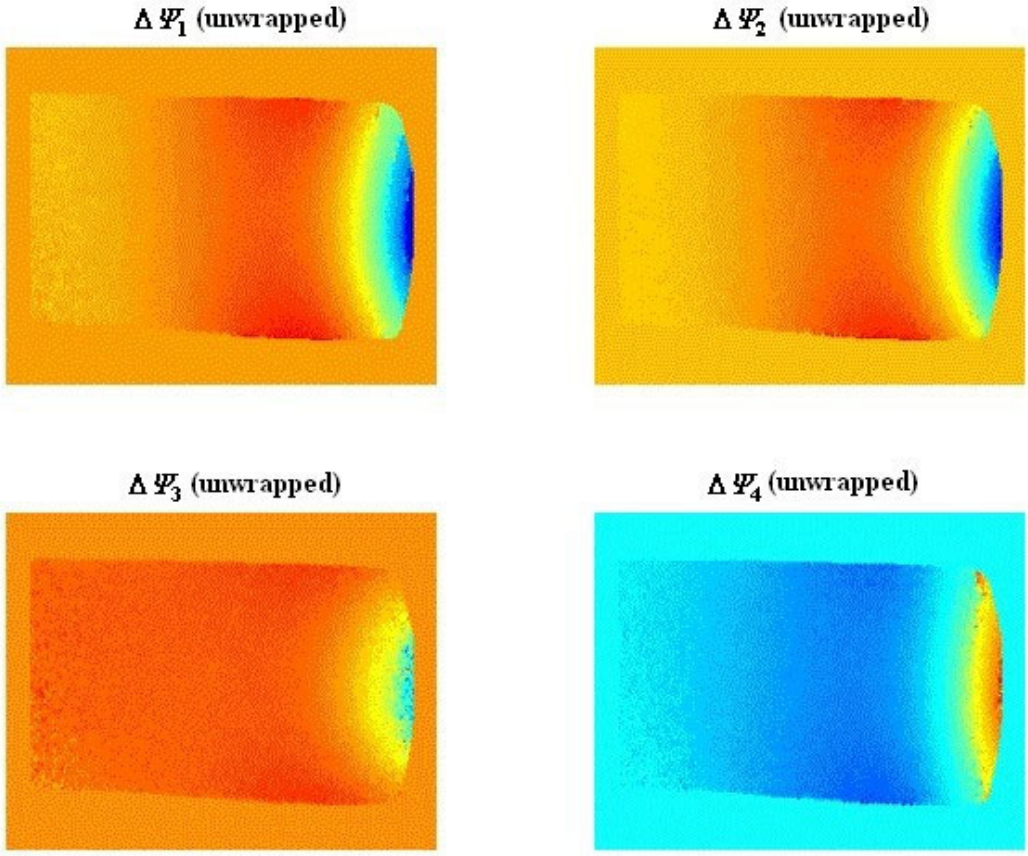

Figure 31 : Unwrapped phase differences

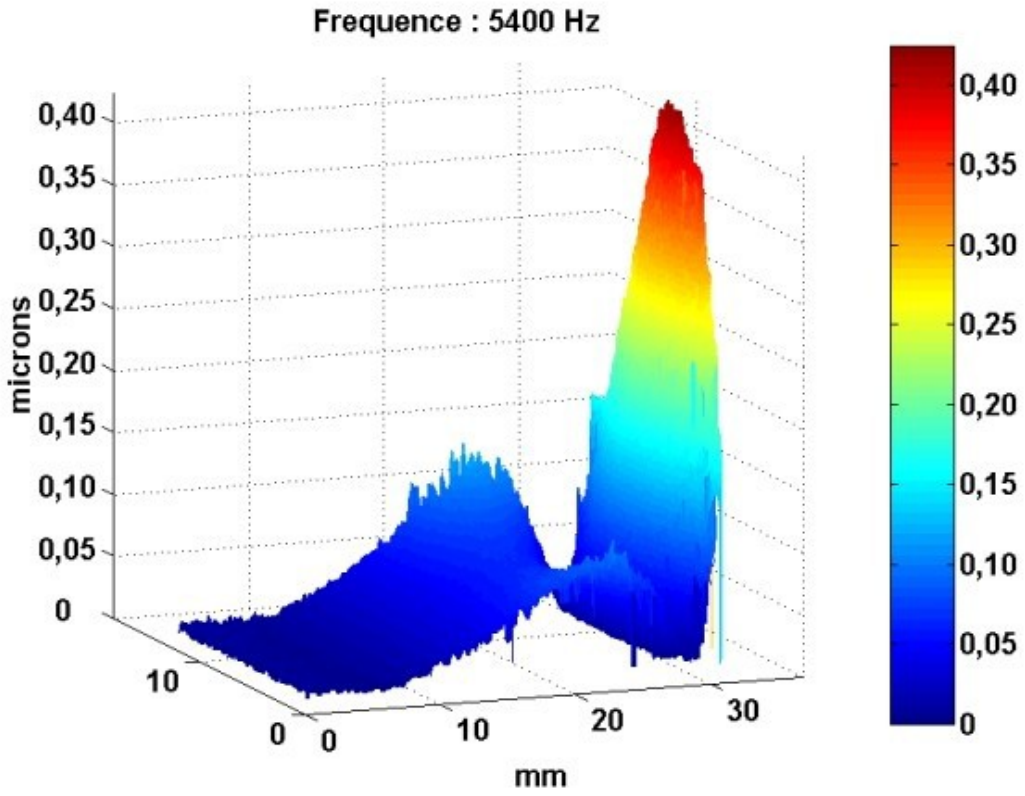

Figure 32 : Vibration amplitude

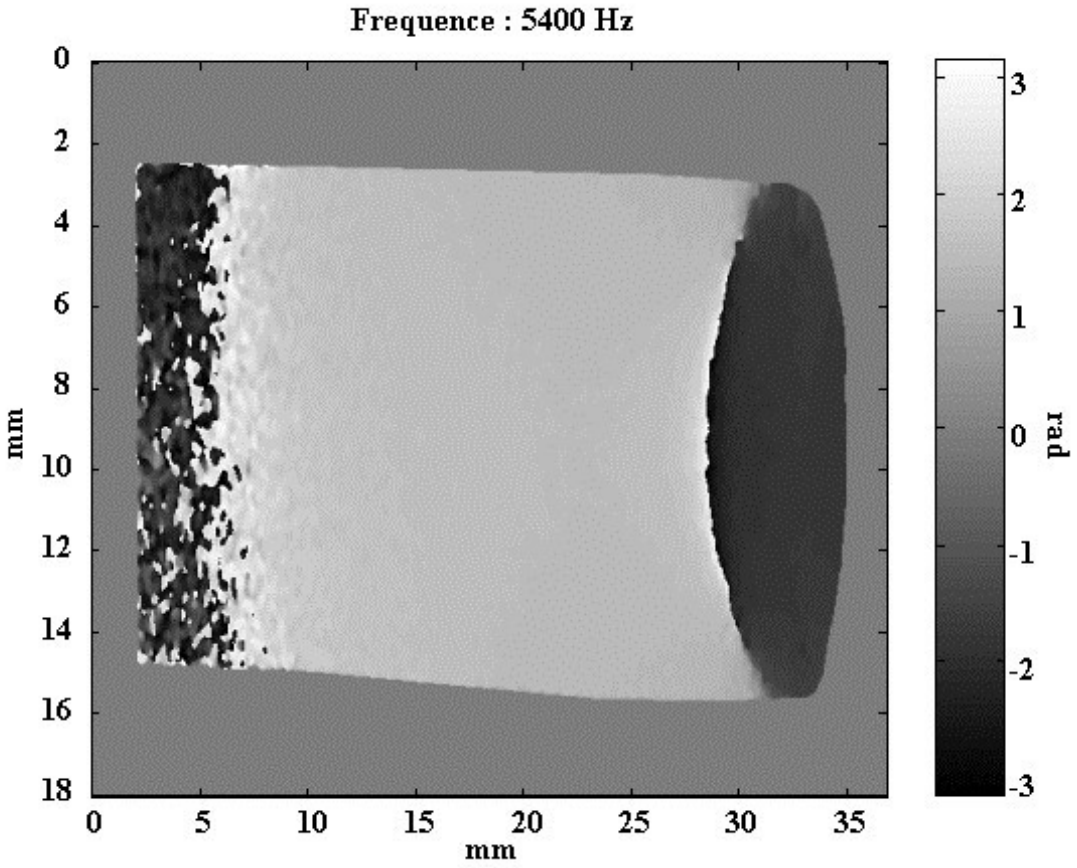

Figure 33 : Vibration phase

Figure 34 is an animation which illustrates the vibration of the reed at 5400 Hz.
Figure 35 is an animation which illustrates the vibration of the reed at 6000 Hz.

* *
*

This course has presented different holographic techniques which take advantage of the remarkable properties of holography. The time averaging techniques are simple but powerful tools in the study of vibrations of structures . However, they don't preserve the vibratory phase and the development of digital holographic vibrometry allows for the amplitude and the phase of the vibration to be simultaneously determined. It should be remembered that digital holographic techniques are normally dedicated to smaller objects because of the lower resolution which is inherent in this technology. Some other methods have not been analysed in this booklet such as those based on the sinusoidal modulation of the reference wave [20 [Phase Evaluation Methods in Whole-Field Optical Measurement Techniques]]. The reader can consult the bibliography to learn more. The methods of holographic interferometry have been the object of numerous developments and applications over the last few years. This course has shown the potential of these methods. If you wish to find a more inexhaustible bibliography on this subject you should consult the works [1 [Holographie Industrielle],2 [Holographic Interferometry – Principles and Methods]].

III.Case study / Exercices

This case study has been designed to illustrate how deformations under mechanical lading are measured using analogic holography. This document is principally made up of questions and answers – that is to say that the exercise section of the course on "Non-contact and optical non-destructive testing applications" can also be found here.

1. Foreword

We propose to study the bending of a cantilever beam, made from Dural steel (Young's modulus $E = 7000\ \text{daN.mm}^{-2}$, density $\varrho = 2500\ \text{kg.m}^{-3}$), of albedo $\varrho_d = 0.2$ and size $L \times h \times e = 150\ \text{mm} \times 5\ \text{mm} \times 25\ \text{mm}$, when a force is applied to its extremity. The retained method is double exposure holographic interferometry using a single reference beam. The optical setup is shown in figure 36.

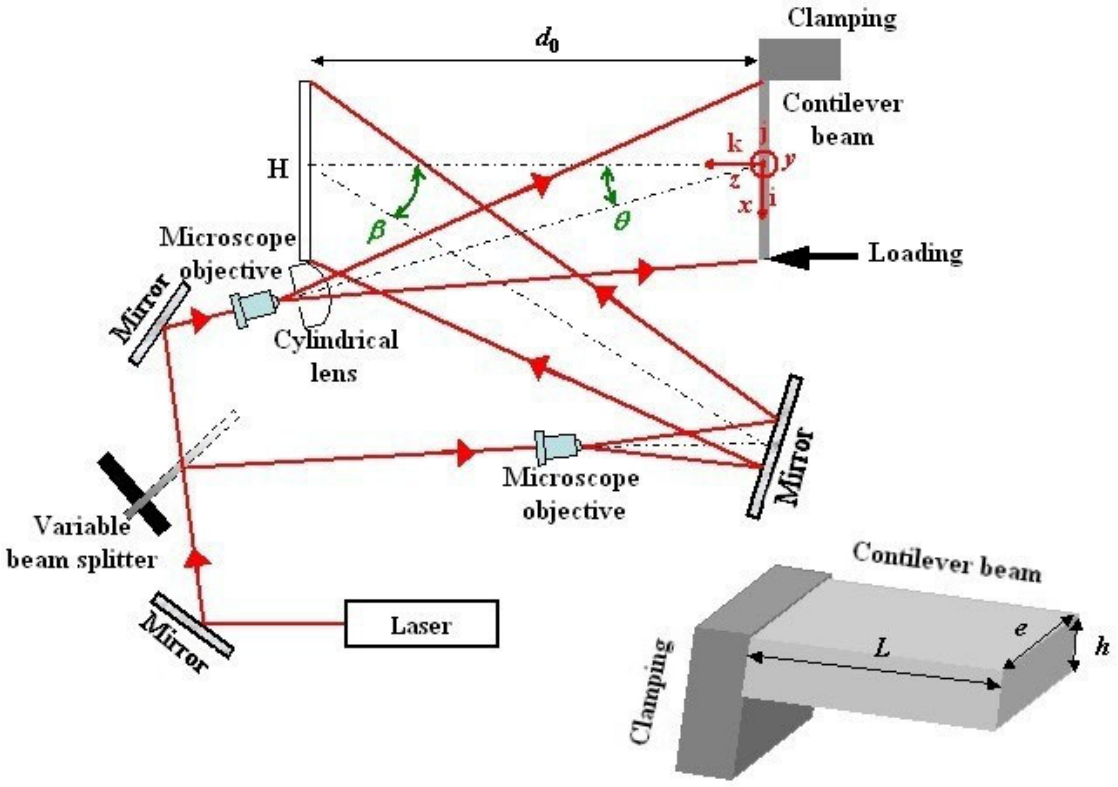

Figure 36 : Study of the cantilever beam of holography

In order to illuminate the beam and to form the reference beam, two microscopic objectives are used. A cylindrical lens placed on the object path allows for the illumination geometry to be adapted to that of the beam. The reference beam is separated from the illumination beam by a beam splitter with variable transmission/reflection.

The laser is a continuous helium-neon laser $(\lambda = 632.8\ \text{nm})$ with power $P_0 = 30\ \text{mW}$. A variable shutter allows for the exposure time of the holgoram to be adjusted. The device is such that $\theta = 30$ and $\beta = 45$. The photosensitive plate used to record the hologram is a photographic emulsion of resolution $3000\ \text{mm}^1$. The reference beam illuminates the entire silver

photosensitive plate with surface $10.16 \times 12.7\ \text{cm}^2$. The photosensitive plate is placed at $d_0 = 1\ \text{m}$ from the object.

2. Self-correcting Exercises

Answer to the following questions

Question 1

[Solution n°1 p 52]

Question 1 : Describe the approach to follow in order to highlight the interference fringes which are characteristic of the deformation of the beam between two states of loading. Draw a diagram of the reconstruction setup which would allow these fringes to be observed.

Question 2

[Solution n°2 p 52]

Question 2 : Is the resolution of the plate sufficient? Up to what average angle between the reference and object beams can the experiment work?

Question 3

[Solution n°3 p 53]

Question 3 : With the use of the sensitivity curve given in figure 39, determine the energy densities W_0 and ΔW so that the recording of the interference fringes is carried out in the linear part of the curve $t = f(W)$. Note W_0 the average density and ΔW the tolerated variation up and down of W_0.

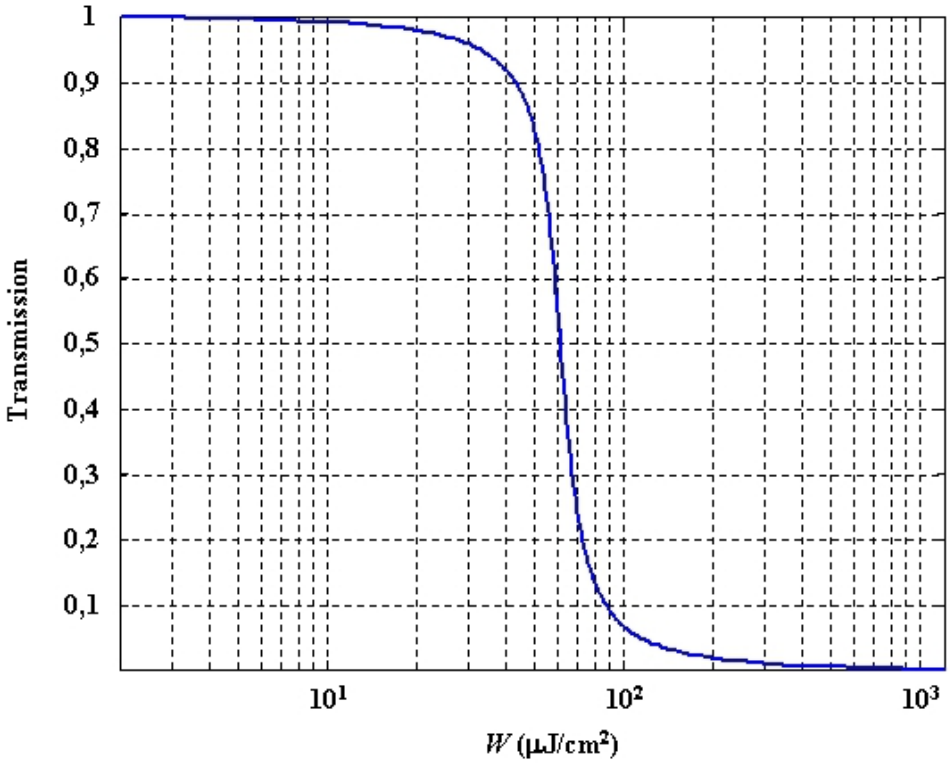

Figure 39 : Sensitivity curve of the emulsion

Question 4

[Solution n°4 p 54]

Question 4 : By noting $a_0$and a_R the amplitudes of the object and reference beams at the holographic plate, determine the ratio a_R/a_0 for W_0 and ΔW in order to assure that the fringes

are recorded in the zone $[W_0 - \Delta W, W_0 + \Delta W]$. From that deduce the ratio of the object and reference beam illuminations E_R/E_0. Discuss the exposure time of the photographic plate. Determine the optical density which would give the user a variable density.

It can be supposed that the power supplied by the laser is shared entirely between the beam (thanks to the cylindric lens) and the holographic plate for the reference beam.

Question 5

[*Solution n°5 p 56*]

Question 5 : By considering the notations in figure 36, express the difference in optical phase between the two exposures. From that, deduce the expression of the interfringe of the beam's iso-displacement lines on the object.

Question 6

[*Solution n°6 p 58*]

Question 6 : The double exposition interferogram of the beam is recorded, photographing the interferogram with the camera during the digital reconstruction stage. The image of the obtained fringes is presented in figure 41.

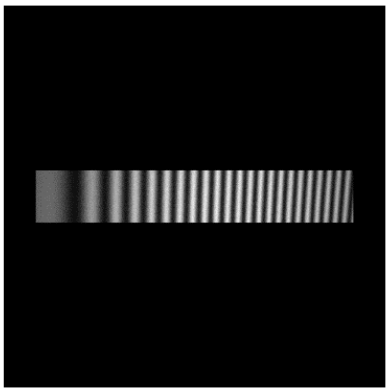

Figure 41 : Interference fringes on the beam in double exposition

What can be said of the way that the force is applied?

The profile of the fringes in the horizontal direction passing through the centre of the beam is represented in figure 42.

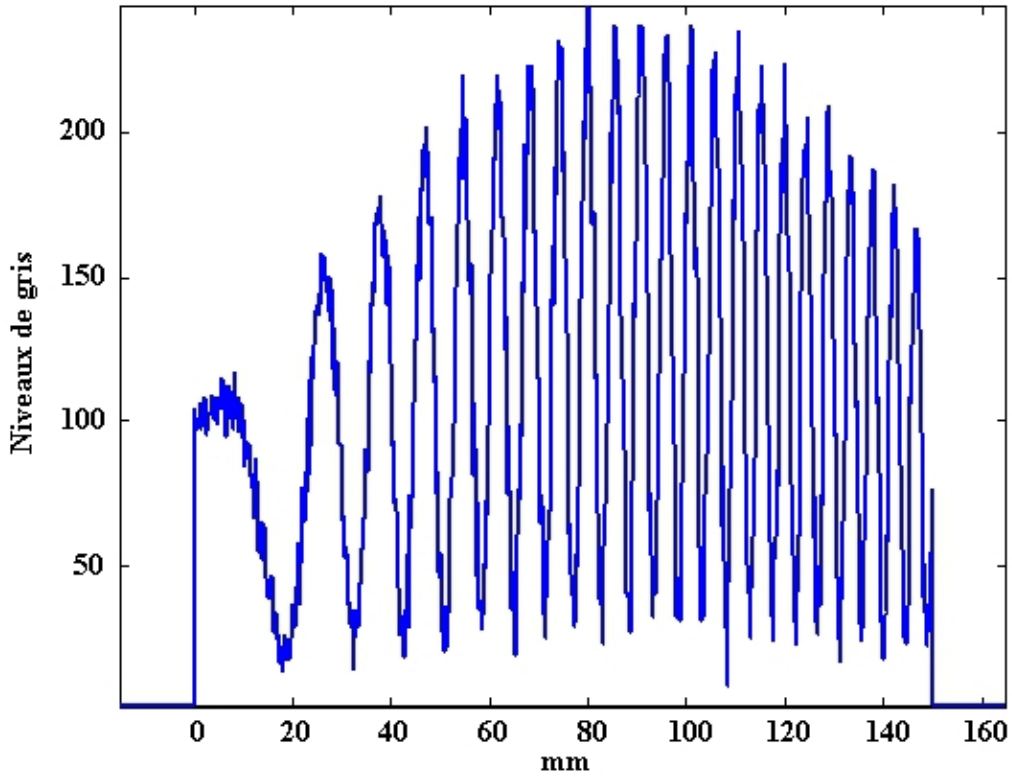

Figure 42 : Profile of the fringes

The position $x = 0$ is registered in relationship to the champing of the beam

In order to obtain a quantitative information on the deformation of the beam, we use the following method :

- we determine the abscissas of the dark fringes of the profile curve
- we calculate the path difference which corresponds to the dark fringes
- from that we deduce the amplitude of the deformation and the bending of the beam at its most extreme point

In order to precisely determine the abscissas of the dark fringes, the profile is digitally processed: the logarithm of the profile is calculated and after a *7 point moving average* low pass filter is applied in order to smooth out the noice. It is thus easier to focus on the center of the dark fringes.

The profile after processing is shown in figure 43

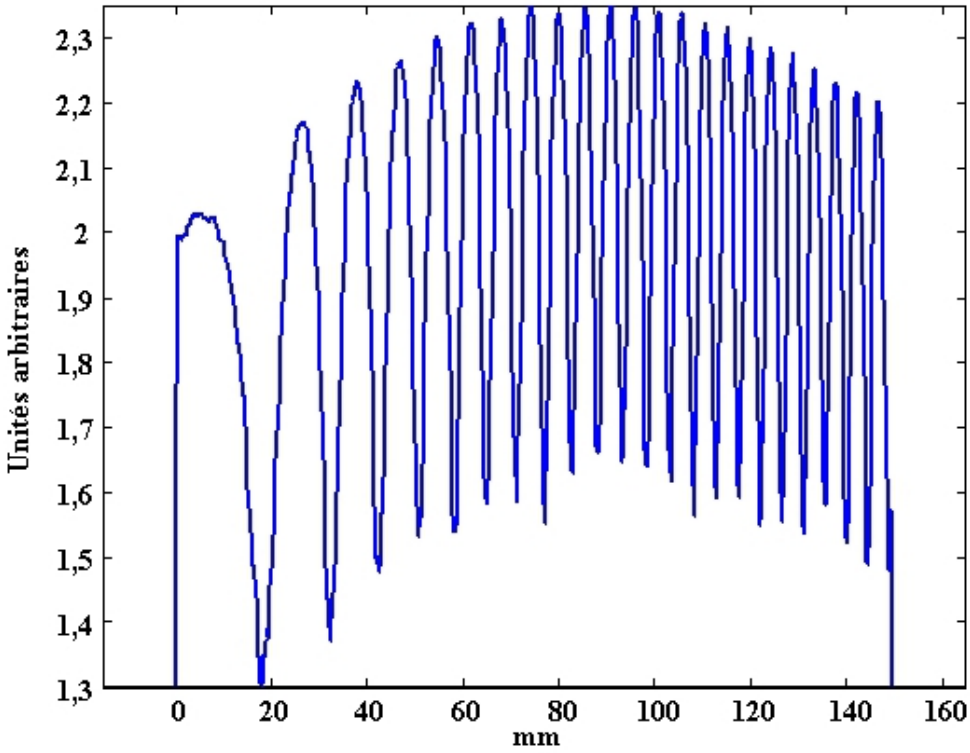

Figure 43 : Profile after processing

By applying the method described above, determine the amplitude an the profile of the deformation.

Question 7

[*Solution n°7 p 61*]

Question 7 : What is the value of the force which is applied to the extremity of the beam?

Question 8

[*Solution n°8 p 62*]

Question 8 : In practice, how can the exposure time of the hologram be estimated?

Solution des exercices

>Solution n°1 *(exercice p. 48)*

The approach to follow in order to highlight the interference fringes which are characteristic of the deformation of the beam between two states is the following :

- a first hologram of the beam at rest is recorded (i.e state 1 : no applied force)
- a force is applied without touching the mounting
- the second hologram is recorded onto the same photoplate after the force has been applied (i.e state 2)

The diagram of the mounting for reconstruction by laser diffraction which would allow the fringes to be observed is shown in figure 37.

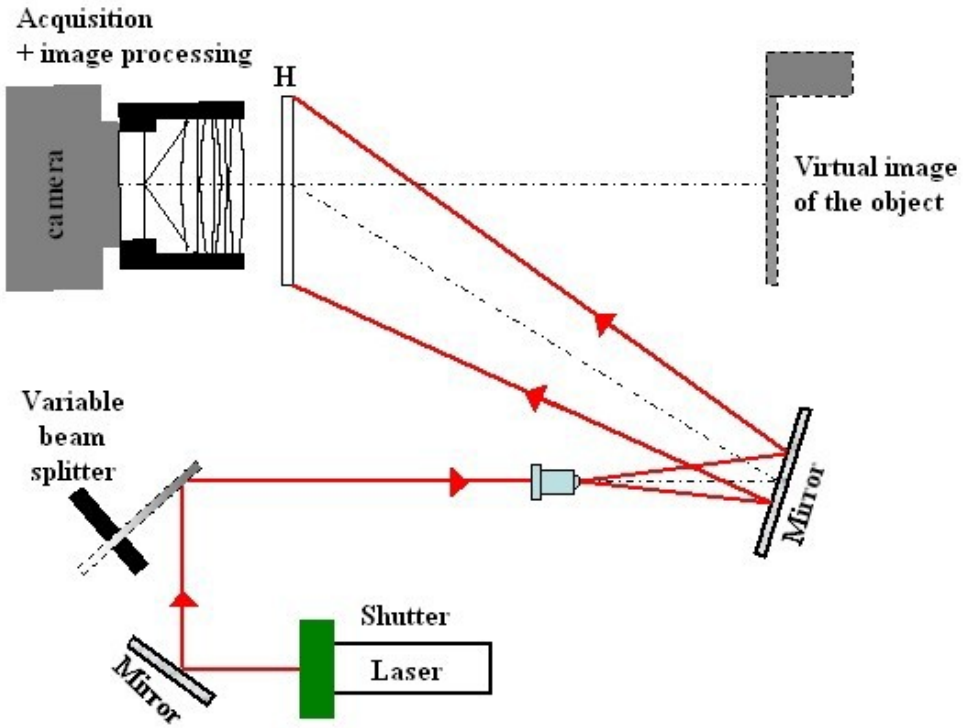

Figure 37 : Reconstruction by laser diffraction

When the hologram is reconstructed by illumination with only the laser, a network of interference fringes are observed on the image of the beam which characterise the bending of the beam. A camera allows for the interferometric image observed in the $+1$-order to be recorded. The analysis off of the fringe network allows for us to quantify the deformation of the beam.

>Solution n°2 *(exercice p. 48)*

Locally, the interfringe of the interference fringes generated by two monochromatic plane waves making an angle β is given by the relationship (see figure 38) :

$$i = \frac{\lambda}{2\sin\left(\frac{\beta}{2}\right)}$$

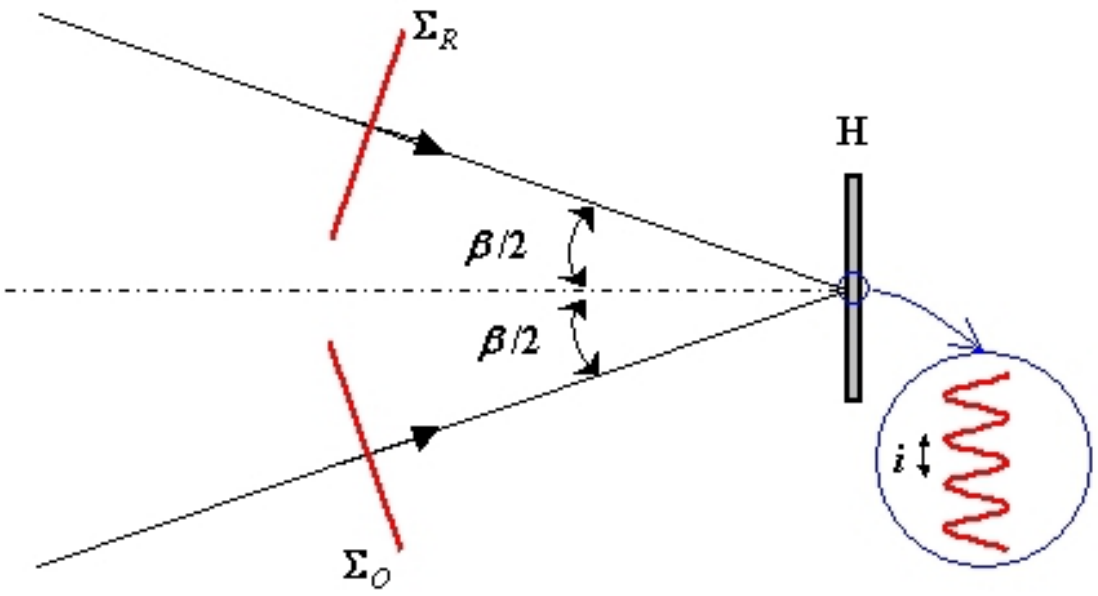

Figure 38 : Interfringe

For $\lambda = 632.8$ nm and $\beta = 45$ we get $i = 0.826\ \mu$m which corresponds to a spatial frequency of $1/0.826 \times 10^{-3} = 1210\ \text{mm}^{-1}$. In order to respect the Shannon criteria, a resolution of at least $2 \times 1210\ \text{mm}^{-1} = 2430\ \text{mm}^{-1}$ is needed. As the resolution of the plate is $3000\ \text{mm}^{-1}$, it is sufficient.

The critical angle is obtained for an interfringe of spatial frequency $3000/2\ \text{mm}^{-1} = 1500\ \text{mm}^{-1}$, that is to say $i = 1/1500 = 0.666\ \mu$m. From that, it is deduced :

$$\beta = 2\ \arcsin\left(\frac{\lambda}{2i}\right) = 2\ \arcsin\left(0\,\frac{,6328}{2\times 0,666}\right) = 56,73\,°$$

The critical angle of incidence for the hologram is 56.73.

>Solution n°3 *(exercice p. 48)*

Question 4 : Figure 40 shows the location of the values to be taken into account.

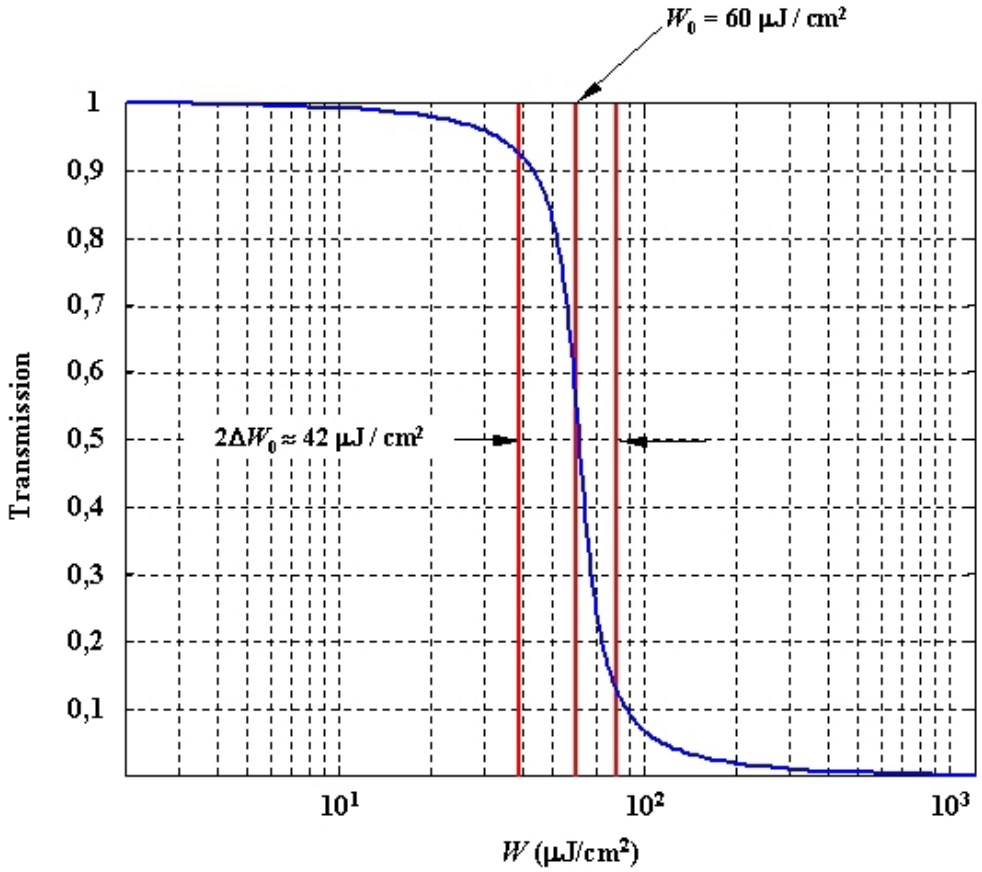

Figure 40 : Determination of sensitivity values

According to figure 40, it can be estimated that $W_0 = 60\,\mu\text{J/cm}^2$ and $\Delta W \approx 21\,\mu\text{J/cm}^2$.

>Solution n°4 *(exercice p. 48)*

To answer this question, we must evaluate the amplitude at the hologram for the object and reference beams.

We note R and T respectively the reflection and transmission factors of the variable beam splitter. We note P_0 and P_R the laser power after the beam splitter for the object and reference beams respectively. We get $R + T = 1$, $P_0 = TP_O$ and $P_R = RP_0$.

The laser illuminance at the object is given by $E_P = P_O/S_P$ where $S_P = L \times e = 15\text{ cm} \times 2.5\text{ cm} = 37.5\text{ cm}^2$ is the illuminated surface. Taking into account that the beam is a diffusing surface, we suppose that it behaves like lambertian diffuser so that its apparent luminance is given by $L_p = \rho_d E_p/\pi = \rho_d P_O/\pi S_p$. Thus, the light power re-emitted from the object to the holographic plate is given by :

$$\Phi_O = L_p G = \frac{\rho_d T P_0}{\pi S_p} \times \frac{S_p S_H}{d_0^2}$$

where $S_H = 10.16 \times 12.7\text{ cm}^2 = 129.16\text{ cm}^2$ is the surface of the holographic plate and $G = S_p S_H/d_0^2$ is the geometric parameter between object and plate.

Thus, the illumination produced by the object beam at the holographic plate is given by

$$E_O = \frac{\Phi_O}{S_H} = \frac{\rho_d T P_0}{\pi d_0^2}$$

The laser illumination supplied at the plate by the reference beam is simply

$$E_R = \frac{R P_0}{S_H}$$

After integration during an exposure time Δt, the interferometric signal at the plate is in the form :

$$H = \Delta t \left(a_R^2 + a_O^2\right) + 2 \Delta t a_R a_O \cos(\varphi)$$

So that the recording is carried out in the linear zone of the sensitivity curve, we must have

$$W_0 = \Delta t \left(E_R + E_O\right)$$

$$\Delta W = 2 \Delta t \sqrt{E_R E_O}$$

The ratio $\Delta W / W_0$ leads to

$$\frac{\Delta W}{W_0} = \frac{2 a_R a_O}{a_R^2 + a_O^2}$$

that is to say

$$\left(\frac{\Delta W}{W_0}\right) a_R^2 - 2 a_R a_O + \left(\frac{\Delta W}{W_0}\right) a_O^2 = 0$$

By looking for $a_R = f(a_O)$, the resolution gives,

$$\frac{a_R}{a_O} = \frac{1 \pm \sqrt{1 - \left(\frac{\Delta W}{W_0}\right)^2}}{\left(\frac{\Delta W}{W_0}\right)}$$

Taking that $\frac{\Delta W}{W_0} = \frac{21}{60} = 0.3525$, this leads to the ratios $\frac{a_R}{a_O} \approx 5.5$ and $\frac{a_R}{a_O} \approx 0.18$. From this we therefore deduce the two possible values for the illumination ratio.

$$\frac{E_R}{E_O} = \frac{a_R^2}{a_O^2} \approx 30$$

$$\frac{E_R}{E_O} \approx 0.032$$

With the illumination expression, we have

$$\frac{a_R}{a_O} = \sqrt{\frac{\pi R d_0^2}{\rho_d T S_H}}$$

The first value of the ratio (30) leads to

$$\frac{R}{T} = 30\frac{\rho_d S_H}{\pi d_0^2} = 30\frac{0.2 \times 129.16}{\pi 100^2} \approx 0.025$$

Since $R + T = 1$, we calculate $T = 1/1.0246 = 0.975$ and $R = 0.024$. In this configuration, the exposure time is given by $\Delta t = W_0/(E_R + E_O)$. The digital calculation leads to :

$$E_R + E_O = \left(\frac{\rho_d T}{\pi d_0^2} + \frac{R}{S_H}\right) P_0 = \left(\frac{0.2 \times 0.975}{\pi 100^2} + \frac{0.024}{129.16}\right) 30000 = 5.76 \ \mu\text{W/cm}^2$$

and from that we deduce the exposure time

$$\Delta t = \frac{60}{5.76} = 10.4 \text{ s}$$

The second value of the ratio (0.032) leads to

$$\frac{R}{T} = 2.63 \times 10^{-5}$$

We find $T = 0.99997$ and $R \approx 2.6 \times 10^{-5}$. In this configuration, the digital calculation leads to

$$E_R + E_O \approx \frac{\rho_d T}{\pi d_0^2} P_0 = 0.19 \ \mu\text{W/cm}^2$$

And from that we deduce the exposure time

$$\Delta t = 315 \text{ s}$$

From the two exposure times, we choose the shortest in order to avoid as much as possible the problems posed by environmental turbulence, $\Delta t = 10.4$ s must therefore be chosen. The optical density of the variable beam splitter is $D = -\log(T) = 0.01$. The reader should not that the reference wave can be generated simply with the vitreous reflection of the laser beam by a glass blade; we also want the ratio E_R/E_O to be large in order to reduce the exposure time of the hologram.

>Solution n°5 *(exercice p. 49)*

The phase difference between the two exposures is given by

$$\Delta\varphi = \frac{2\pi}{\lambda}\mathbf{U}.\mathbf{S}$$

where $\mathbf{U}$ is the vector of the object's displacement between the two exposures. Considering that the beam is fixed in place and that its displacement is weak, we get $\mathbf{U} \approx u_z\mathbf{k}$. The and observation vectors are :

$$\mathbf{K_e} = -\sin\theta\,\mathbf{i} - \cos\theta\,\mathbf{k}$$

$$\mathbf{K_o} = \mathbf{k}$$

The sensitivity vector is them :

$$\mathbf{S} = \mathbf{K_e} - \mathbf{K_o} = -\sin\theta\,\mathbf{i} - (1+\cos\theta)\,\mathbf{k}$$

Hence

$$\Delta\varphi = -\frac{2\pi}{\lambda}(1+\cos\theta)u_z$$

Remarque

The negative sign of this expression indicates that for a positive displacement in the direction of the vector *k*, the phase variation between the two states will be negative. This is coherent with the notations chosen in figure 36 since the optical path *source-object-plate* reduces when the object is under stress (its edge gets closer to the plate).

Remarque

The illumination vector considered in the calculation is an average illumination vector, that is to say that it corresponds to the illumination direction of the average object illumination beam ; however, in the setup the illumination beam is divergent and therefore the sensitivity vector depends on the point on the object being considered ; strictly this vector varies in the field of viewand it is logically necessary to take that into account when calibrating.

The interfringe of the object's iso-displacement lines is obtained for a phase variation of 2π between two consecutive fringes of the same nature (white or dark). Note Δu_z which is this interfringe.

We have

$$\Delta\varphi_k = -\frac{2\pi}{\lambda}(1+\cos\theta)u_z = 2k\,\pi$$

$$\Delta\varphi_{k-1} = -\frac{2\pi}{\lambda}(1+\cos\theta)(u_z+\Delta u_z) = 2(k-1)\,\pi$$

Hence

$$\Delta u_z = \frac{\lambda}{1+\cos\theta}$$

The numerical application gives $\Delta u_z = 0.6328/(1+\cos 30) = 0.339\,\mu\text{m}$

>Solution n°6 *(exercice p. 49)*

By observing the interferogram, it is noticed that the fringes at the end of the beam are slightly tilted in relation to the vertical direction. Strictly speaking, when the object bends, the fringes should stay parallel to the vertical. Since they are not perfectly parallel, it can be deduced that the force has not been applied to the central axis of the object but that the pressure has been applied slightly off-centre. It should be noted that the sensitivity of the interferometric method allows us to verify whether the mechanical test has been correctly carried out.

In figure 44, the dark fringes and their abscissa have been plotted. 23 dark fringes can be counted starting from the champing. At $x = 0$, the fringe is white and the deformation is null at the champing. Between the white fringe at 0 and the first dark fringe the path difference is $\Delta u_x/2 = 0.169\ \mu\text{m}$, and between each dark fringe it is $\Delta u_z = 0.339\ \mu\text{m}$.

The score of the fringes is shown in table 3.

n° fronge	x (mm)
0	0
1	18
2	32
3	43
4	51
5	58
6	65
7	72
8	77
9	83
10	88
11	94
12	99
13	103
14	108
15	113
16	118
17	122
18	127
19	131
20	136
21	140
22	144
23	149

Table 3 : Relationship between the number of dark fringes / abscissa of the fringe

From the values in the table the deformation of the object is deducted (table 4) and its profile is given in figure 45. The force is applied in a positive direction, so the deformation is therefore positive. The phase variation has not been evaluated but its signal is negative. Considering the information given above

With digital values, the maximum deformation is estimated at about $u_z^{max} = 7.63\ \mu\text{m}$.

x (mm)	u_L (µm)
0	0
18	0,17
32	0,51
43	0,85
51	1,19
58	1,53
65	1,87
72	2,2
77	2,54
83	2,88
88	3,22
94	3,56
99	3,9
103	4,24
108	4,58
113	4,92
118	5,26
122	5,6
127	5,93
131	6,27
136	6,61
140	6,95
144	7,29
149	7,63

Table 4 : Relationship between abscissa of the fringe / object's displacement

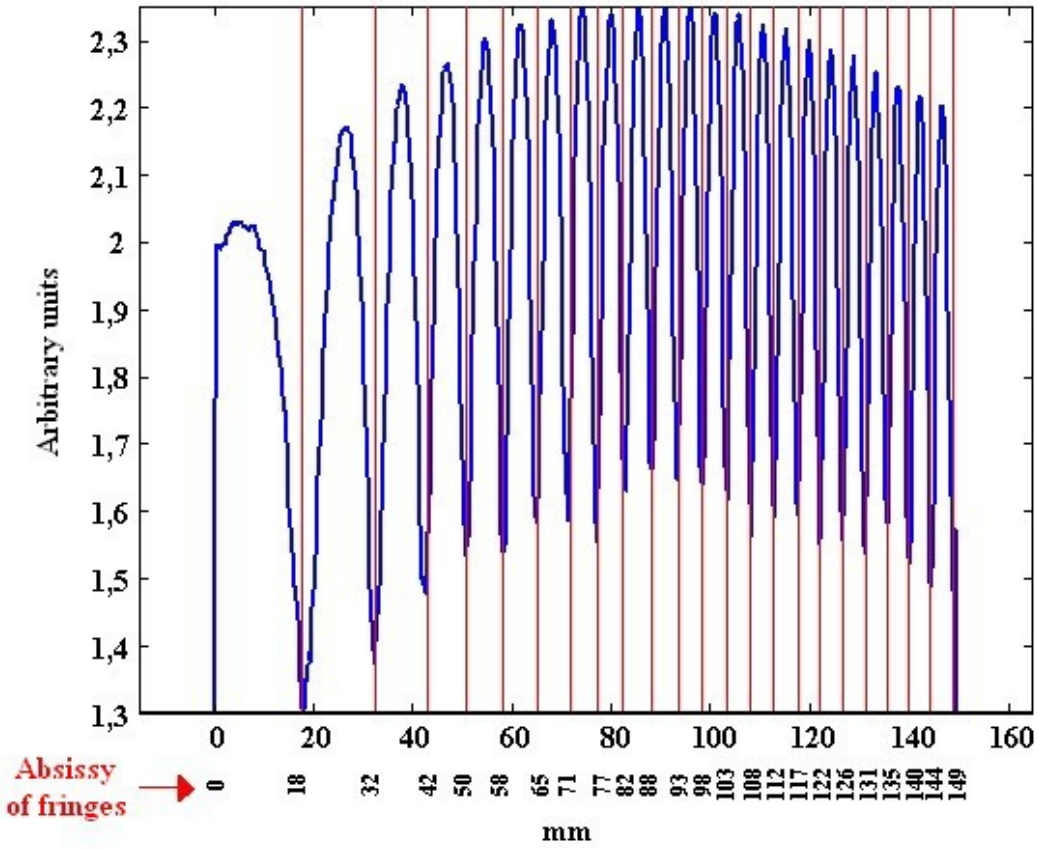

Figure 44 : Dark fringes

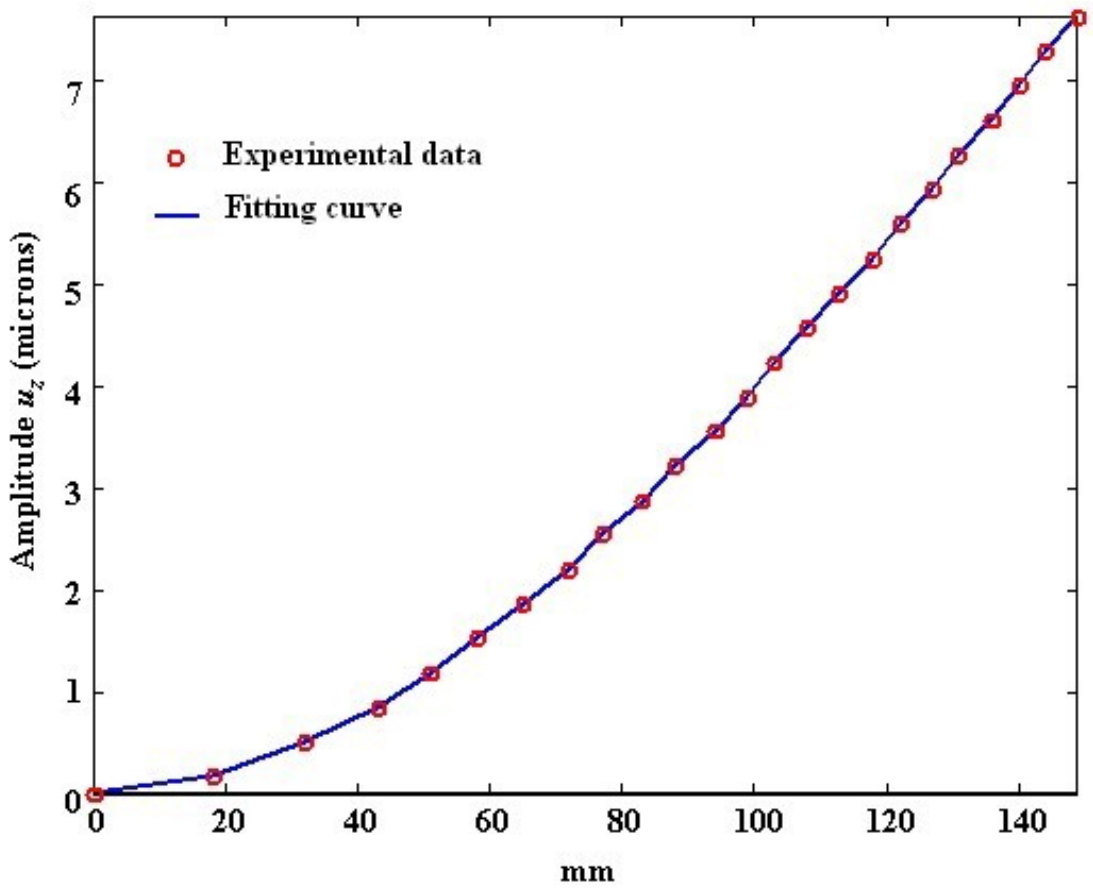

Figure 45 : Profile of the objects deformation

>Solution n°7 *(exercice p. 51)*

The displacement is given by the following relationship [21 [Use of Modulated Reference Wave in Electronic Speckle Pattern Interferometry]] :

$$u_z(x) = \frac{2FL^3}{Eeh^3}\left(\frac{x}{L}\right)^2\left(3-\frac{x}{L}\right)$$

At the end of the beam $x = L$ and $u_z(L) = 4FL^3/Eeh^3$. Since $u_z(L) = u_z^{max}$, we find

$$F = \frac{Eeh^3u_z^{max}}{4L^3} = \frac{7000\times25\times5^3\times7.63\times10^{-3}}{4\times150^3} = 0.0125\ N$$

Remarque

It should be remarked that: we have just determined that the applied force is in the 10^{-3} Newton range. This force has generated several resolved fringes on the beam (23 were counted) ; a greater force would have generated fringes which were too tightly packed to be observed ; thus, so that the methods of holographic interferometry are applicable to experimental mechanics, the amplitude of the force applied to the structure must be perfectly controlled in a way as to be capable to analyse the fringes in order to get a quantification of them.

>Solution n°8 *(exercice p. 51)*

The photometric evaluation which has been proposed is not ideal as we have not taken into account the losses due to the optical elements and to the fact that the beams do not perfectly illuminate the optical and mechanical elements. However, this evaluation remains realistic because the size of the calculated exposure time conforms to what we would estimate in practice with equivalent setup and laser. In practice, the exposure time is directly estimated from the mesurement of object and reference illumination at the hologram plane. Putting this into practice is simple: a light meter is used and the illumination given by the reference beam is measured followed by the illumination given by the object beam. It is checked that the two values are in the right ration which is imposed by the characteristics of the recording plate (in this case study we have $E_R/E_O \approx 30$). If the beams are not in the right ratio, they can be adjusted with the help of the variable beam splitter. Having carried out the adjustment, the illumination values given by the aparatus in lux must be converted into **energy units** in $\mathrm{W.m^{-2}}$. To do this, the conversion factor at the laser wave length must be known. Finally, the relationship $\Delta t = W_0/(E_R + E_O)$ is applied in order to estimate the exposure time.

Bibliographie

[A Determination of the Optimum Beam Ratio to Produce Maximum Contrast Photographic Reconstructions from Double-Exposure Holographic Interferograms] Sollid J.E., Swint J.B., *A Determination of the Optimum Beam Ratio to Produce Maximum Contrast Photographic Reconstructions from Double-Exposure Holographic Interferograms* (p.pp 2717-2719), Applied Optics, 1970--, Vol. 9, .

[Dual and Multiple Beam Interferometry by Wavefront Reconstruction] Burch J.M., Ennos A.E., Wilton R.J., *Dual and Multiple Beam Interferometry by Wavefront Reconstruction* (p.pp 1015-1016), Nature, 1966--, Vol. 209, .

[Dynamic Modal Characterization of Musical Instruments Using Digital Holography] Demoli N., Demoli I., *Dynamic Modal Characterization of Musical Instruments Using Digital Holography* (p.pp 4812-4817), Optics Express, 2005--, Vol. 13, .

[Fringe Interpolation by Two-Reference-Beam Holographic Interferometry : Reducing Sensitivity to Hologram Misalignment] Dandliker R., Thalmann R., Willemin J.F., *Fringe Interpolation by Two-Reference-Beam Holographic Interferometry : Reducing Sensitivity to Hologram Misalignment* (p.pp 301-306), Optics Communications, 1982--, Vol. 42, .

[Full Field Vibrometry With Digital Fresnel Holography] Leval J., Picart P., Boileau J.-P., Pascal J.C., *Full Field Vibrometry With Digital Fresnel Holography* (p.pp 5763-5771), Applied Optics, 2005--, Vol. 44, n° N°27, .

[Holographic Interferometry] Bazergui A., *Holographic Interferometry*, Ecole Polytechnique de Montréal, Montréal, 1993.

[Holographic Interferometry Applied to Measurements of Small Static Displacement of Diffusely Reflecting Surfaces] Sollid J.E., *Holographic Interferometry Applied to Measurements of Small Static Displacement of Diffusely Reflecting Surfaces* (p.pp 1587-1595), Applied Optics, 1969--, Vol. 8, .

[Holographic Interferometry – Principles and Methods] Kreis Thomas, *Holographic Interferometry – Principles and Methods*, Akademie Verlag, Berlin, 1996.

[Holographie Industrielle] Smigielski Paul, *Holographie Industrielle*, Teknéa, Toulouse, 1994.

[Interferometric Analysis by Wavefront Reconstruction] Powell R.L., Stetson K.A., *Interferometric Analysis by Wavefront Reconstruction* (p.pp 1593-1598), Journal of the Optical Society of America, 1965--, Vol. 55, n° N°12, .

[Interferometric Measurements on Diffuse Surfaces by holographic Techniques] Haines K.A., Hildebrabd B.P., *Interferometric Measurements on Diffuse Surfaces by holographic Techniques* (p.pp 595-602), Applied Optics, 1966--, Vol. 5, .

[Interferometry With a Holographically Reconstructed Comparison Beam] Brooks R.E., Heflinger L.O., Wuerker R.F., *Interferometry With a Holographically Reconstructed Comparison Beam* (p.pp 248-249), Applied Physics Letters, 1965--, Vol. 7, .

[Phase Evaluation Methods in Whole-Field Optical Measurement Techniques] Dorrio B.V., Fernandez J.L., *Phase Evaluation Methods in Whole-Field Optical Measurement Techniques* (p.pp 33-55), Measurement Science and Technology, 1999--, Vol. 10, .

[Phase Measurement Interferometry Techniques] Creath K., *Phase Measurement Interferometry Techniques* (p.pp 349-393), Progress in Optics, 1988--, Vol. XXVI, .

[Principle of Optics] Born Max, Wolf Emil, *Principle of Optics*, Pergamon Press, New York, 1959.

[Pulsed Digital Holography Combined With Laser Vibrometry for 3D Measurements of Vibrating Objects] Pedrini G., Schedin S., Tiziani H.J., *Pulsed Digital Holography Combined With Laser Vibrometry for 3D Measurements of Vibrating Objects* (p.pp 117-129), Optics and Lasers in Engineering, 2002--, Vol. 38, .

[Some Opportunities for Vibration Analysis with Time-Averaging in Digital Fresnel Holography] Picart P., Leval J., Mounier D., Gougeon S., *Some Opportunities for Vibration Analysis with Time-Averaging in Digital Fresnel Holography* (p.pp 337-343), Applied Optics, 2005--, Vol. 44, n° N°3, .

[Time-Averaged Digital Holography] Picart P., Leval J., Mounier D., Gougeon S., *Time-Averaged Digital Holography* (p.pp 1900-1902), Optics Letters, 2003--, Vol. 28, n° N°20, .

[Time-Averaged In-Line Digital Holographic Interferometry for Vibration Analysis] Asundi A., Singh V.R., *Time-Averaged In-Line Digital Holographic Interferometry for Vibration Analysis* (p.pp 2391-2395), Applied Optics, 2006--, Vol. 45, .

[Two-Reference-Beam Holographic Interferometry] Dandliker R., Marom E., Mottier F.M., *Two-Reference-Beam Holographic Interferometry* (p.pp 23-30), Journal of the Optical Society of America, 1976--, Vol. 66, .

[Use of Modulated Reference Wave in Electronic Speckle Pattern Interferometry] Lokberg O.J., Hogmoen K., *Use of Modulated Reference Wave in Electronic Speckle Pattern Interferometry* (p.pp 847-851), Journal of Physics E : Scientific Instruments, 1976--, Vol. 9, .